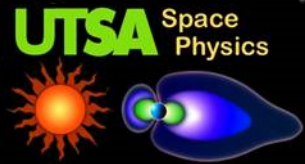


An Observational Study of the Relationship Between Precipitating Ions and Energetic Neutral Atoms (ENA's) Emerging From the Ion/Atmosphere Interaction

David Mackler
Postdoctoral Researcher
Goddard Space Flight Center



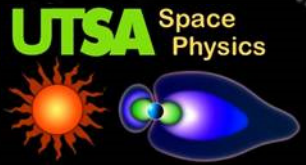
Outline of Topics



- Objective
- Introduction
- Data Analysis
- Results
 - LAE Geomagnetic Index Correlation
 - LAE/In Situ Response to Storms
 - LAE/In Situ Correlation
 - LAE/In Situ Comparison



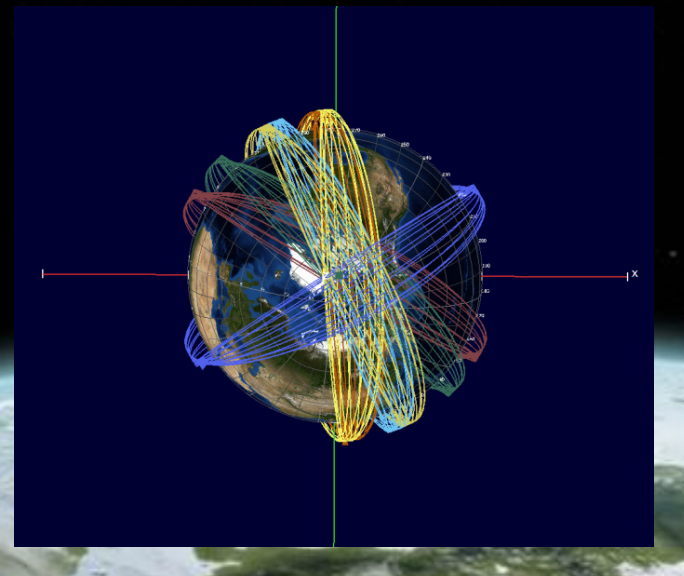
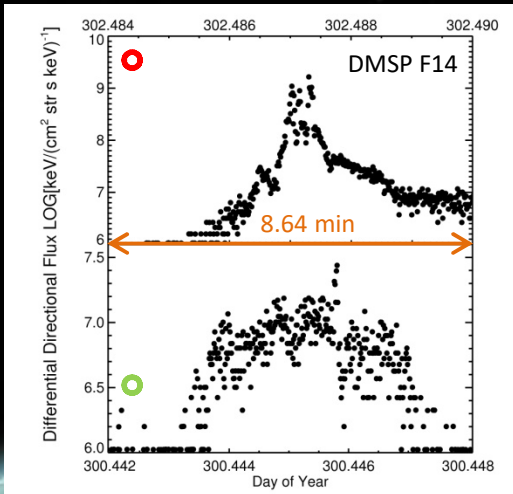
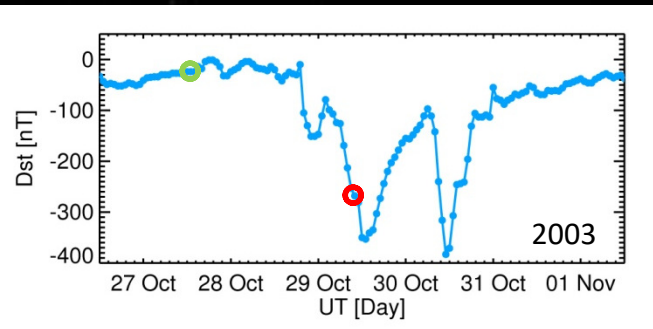
Objective



Further the understanding of the energy injected into the terrestrial atmosphere by plasma sheet ions during geomagnetic storms using Energetic Neutral Atom (ENA) imaging.

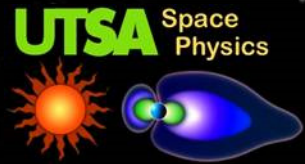
In Situ Measurement of Ion Precipitation

- Orbit ~100 minutes; Passes a precipitation region in ~5+ minutes
- Limited local time coverage:
 - Sun Synchronous





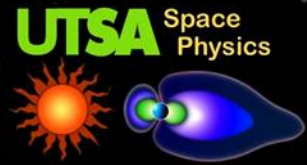
Outline of Topics



- Objective
- Introduction
- Data Analysis
- Results
 - LAE Geomagnetic Index Correlation
 - LAE/In Situ Response to Storms
 - LAE/In Situ Correlation
 - LAE/In Situ Comparison



Energetic Neutral Atoms (ENAs)



Magnetospheric ENAs

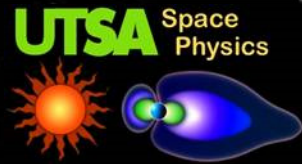
- Higher energy than ionospheric neutrals
 - 1-100s keV
- Created by charge exchange of precipitating ions with cold exospheric neutrals (oxygen exobase)
- Low Altitude Emission (LAE) – associated with high latitude footprints of Earth's magnetosphere (most intense ENAs)
- Problem: LAEs are outside the loss cone and are not precipitating ions

Do LAEs behave similarly to ion precipitation during geomagnetic activity?



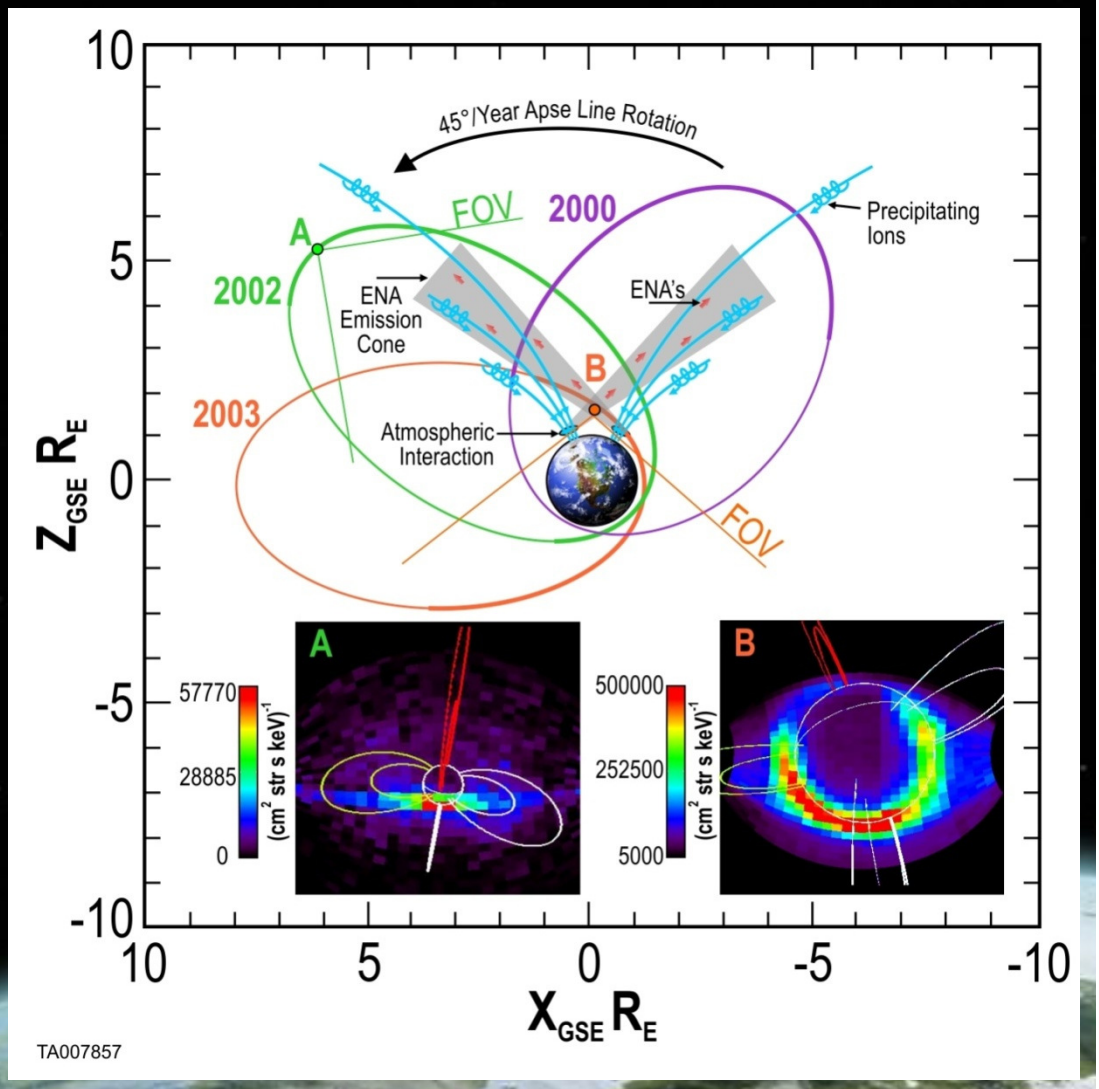


Geomagnetic Emission Cone



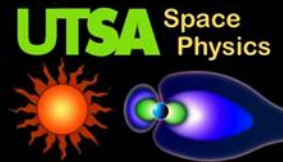
- Observed LAEs are highly anisotropic; ENAs near mirror point
- Pitch angle slightly larger than 90° is preferential to escape
 - Escape angle
- Observation location
 - Determines local time distribution
 - Far: opposite hemisphere

Statistics!





Geomagnetic Emission Cone



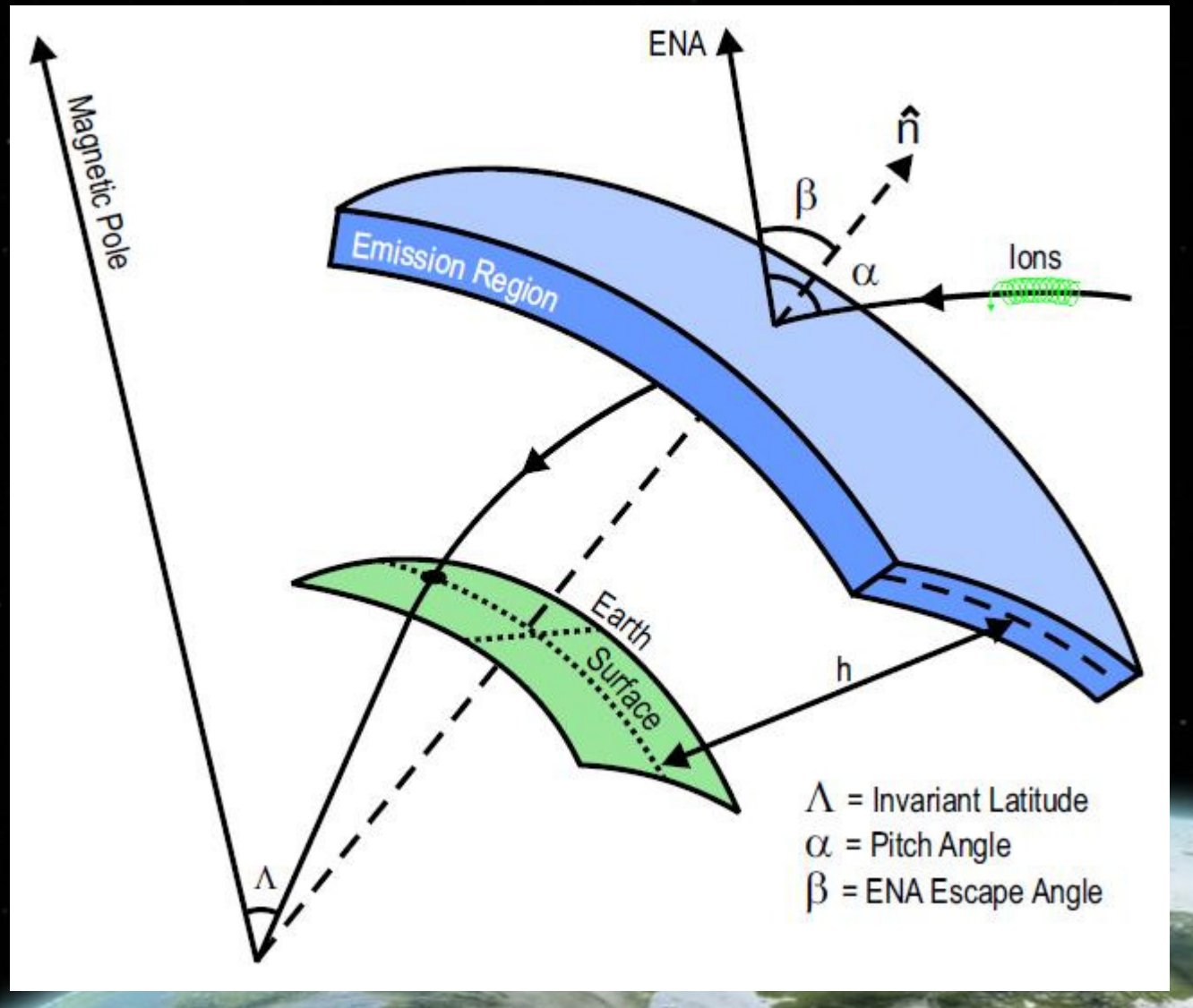
Corollary – Escape Angle

Escape Angle (β)
vs. Pitch Angle (α)

α : Tied to the
Magnetic Field

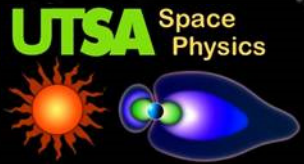
β : Associated with
the Local
Atmosphere

ENA Escape Angle
may be preferential
to ‘thinnest’ path





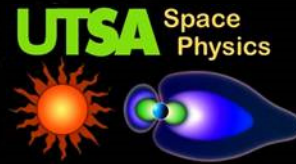
Outline of Topics



- Objective / Merits of the Study
- Introduction
- Data Analysis
- Results
 - LAE Geomagnetic Index Correlation
 - LAE/In Situ Response to Storms
 - LAE/In Situ Correlation
 - LAE/In Situ Comparison



IMAGE Mission



Imager for Magnetopause-to-Aurora Global Exploration

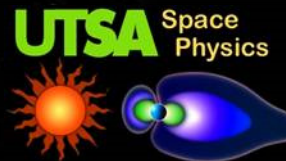
IMAGE used neutral atom, ultraviolet, and radio imaging techniques to:

- Identify the dominant mechanisms for injecting plasma into the magnetosphere on substorm and magnetic storm time scales;
- Determine the directly driven response of the magnetosphere to solar wind changes; and,
- Discover how and where magnetospheric plasmas are energized, transported, and subsequently lost during substorms and magnetic storms.



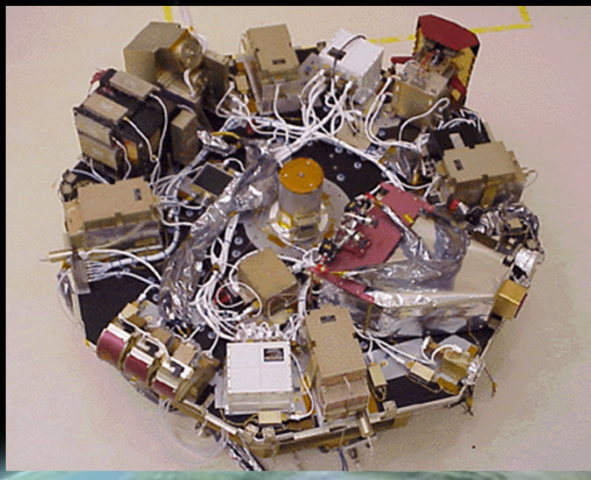
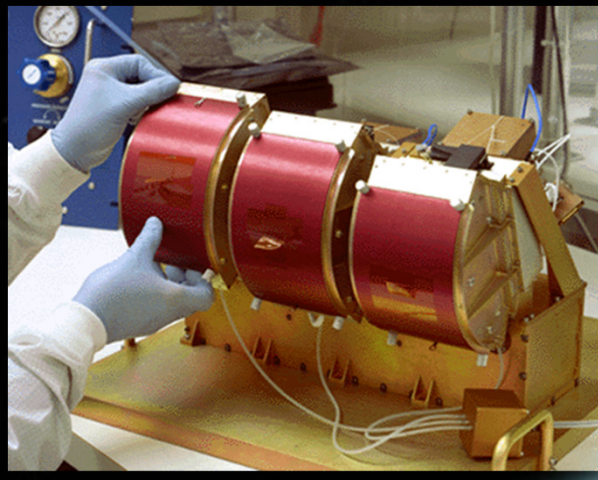
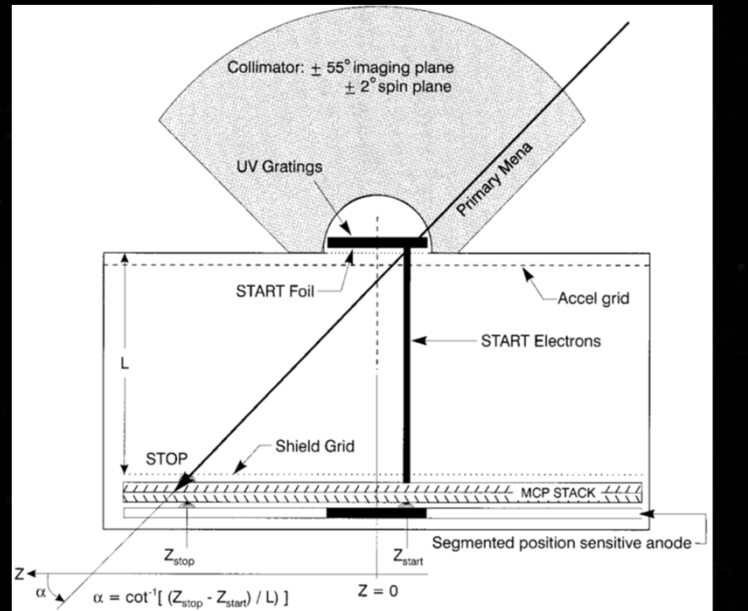


IMAGE Mission



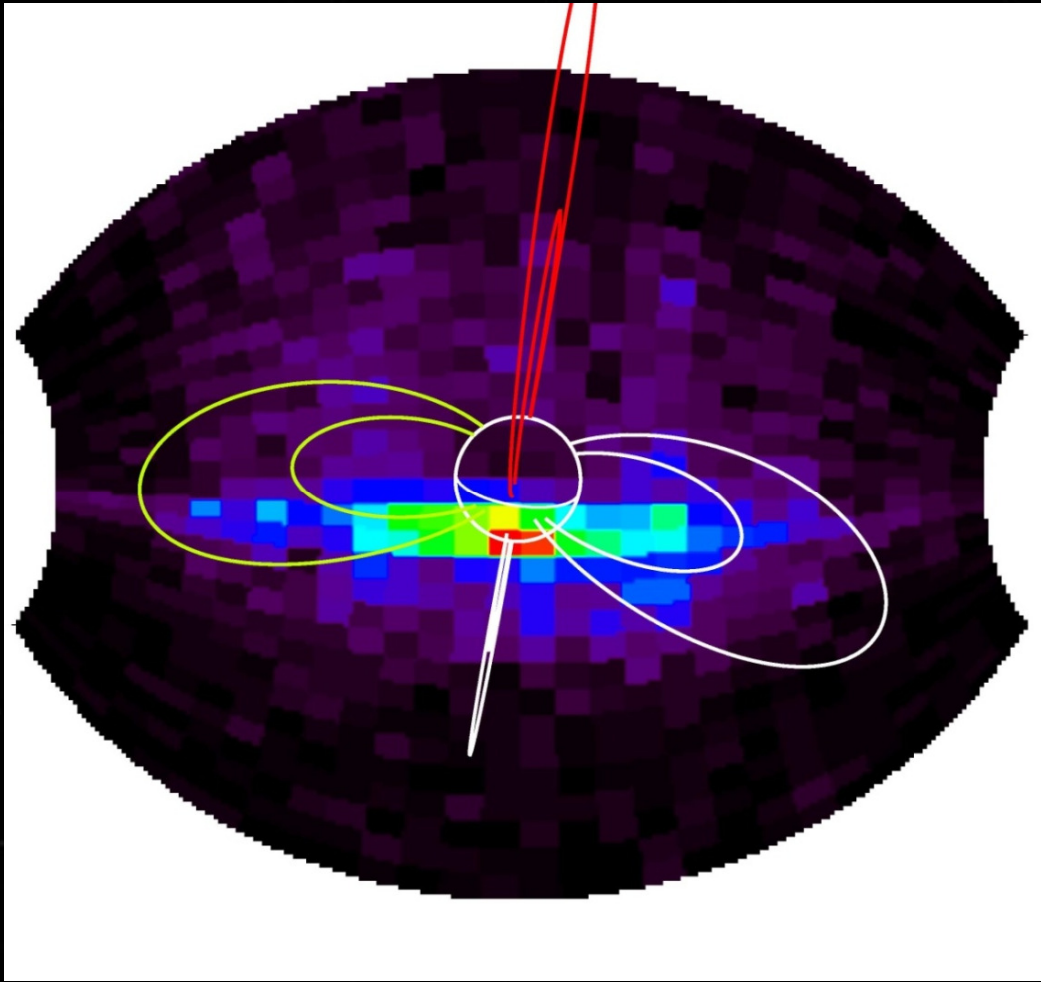
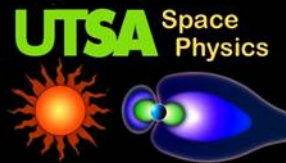
Medium Energy Neutral Atom Imager

- Pinhole camera
- 3 heads combined
- 1 – 30 keV
- 2 minutes per image
- Data from 2000 - 2005





MENA Data



Medium Energy Neutral Atom Imager

Energy: ~1-30 keV

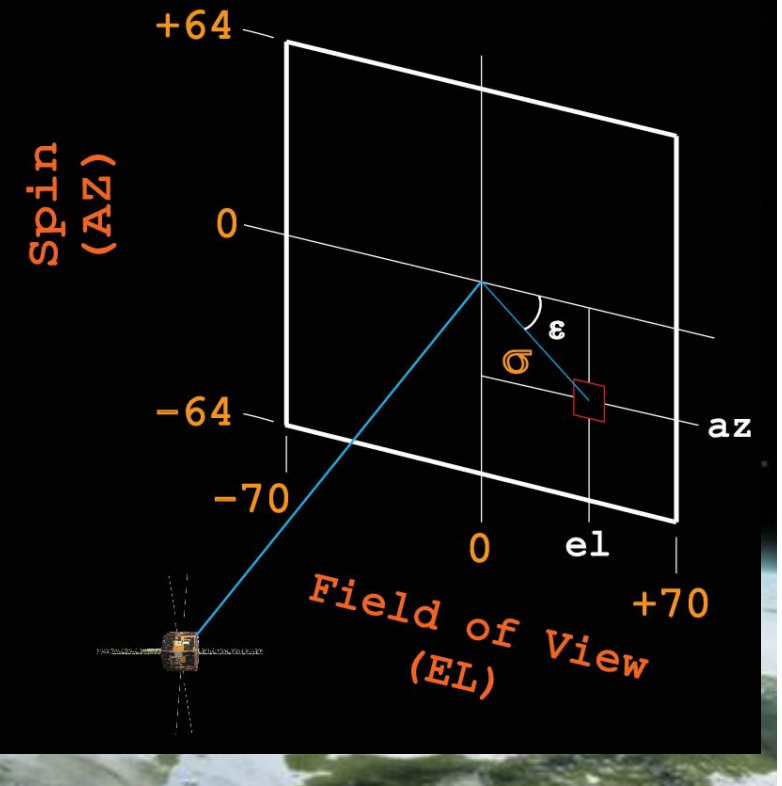
- Using ~1-12 keV

Pixel size

- AZ: 4° (32 pixels)
- EL: 5° (28 pixels)

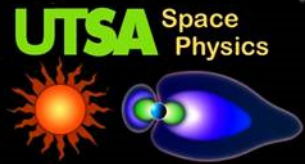
Sigma

- Angular ‘distance’ from center

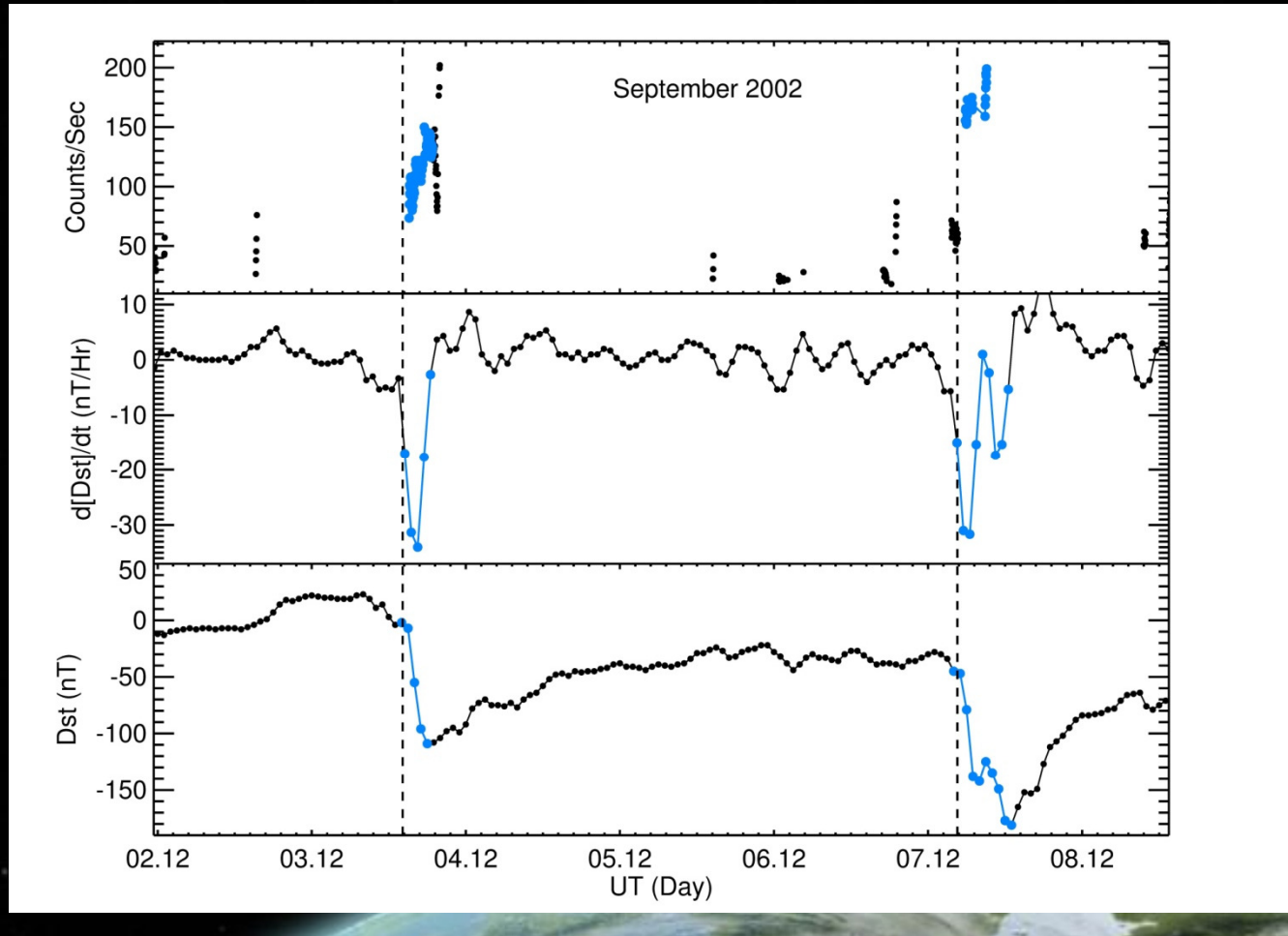




Data Analysis – LAE Dataset



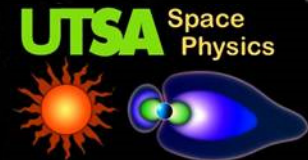
- LAE images are manually selected from MENA dataset
- Reality check: Just using LAE dataset and Dst





Data Analysis – Initial Points Collection

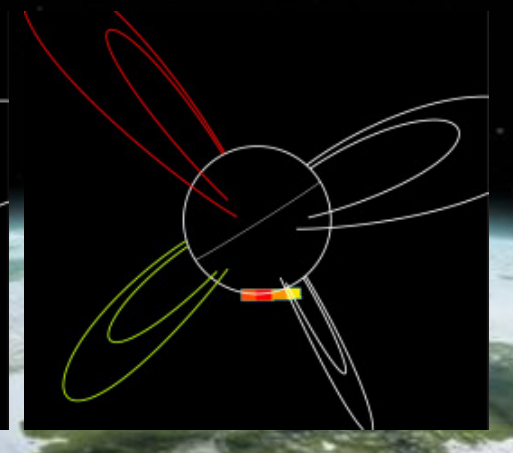
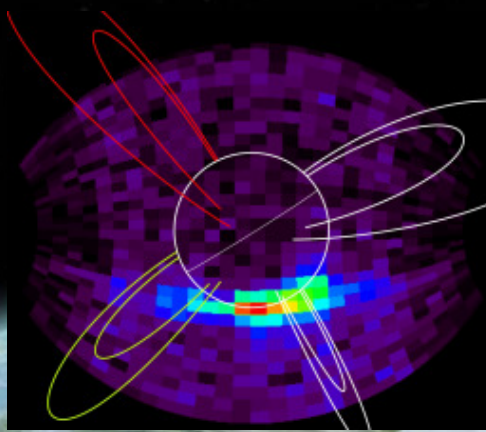
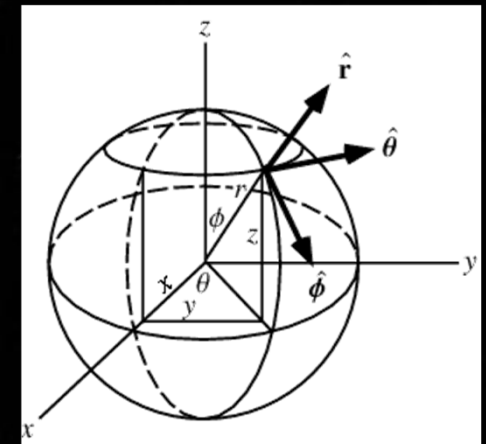
“Batch” Processor



Goal: Collect pixel coordinates and B field for four corners and center of LAE pixels

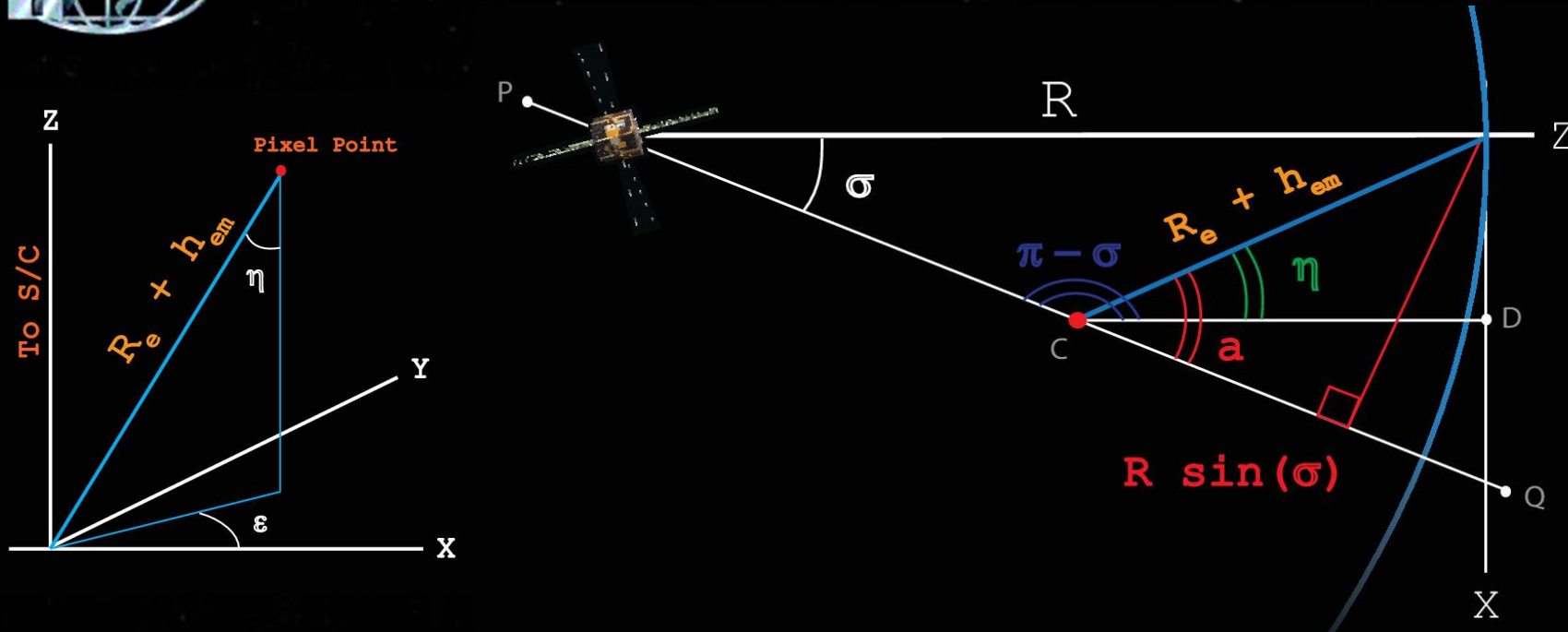
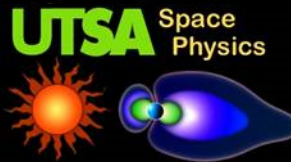
- Only consider pixels with a corner within $R_e + h$
- Integrate over low three energy bins (1 - 12.1 keV)
- Keep pixels most associated with LAEs
- Assume spherical emission region
 - Project pixel to a sphere of radius $R_e + h$
- Use the IGRF to find B

S/C





Data Analysis – Initial Points Collection



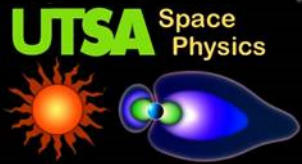
$$\eta = [\pi - \text{sigma}] - \left[\pi - \sin^{-1} \left(\frac{R \cdot \sin[\text{sigma}]}{R_e + h} \right) \right]$$

$$\varepsilon = \tan^{-1} (az_sample / el_sample)$$

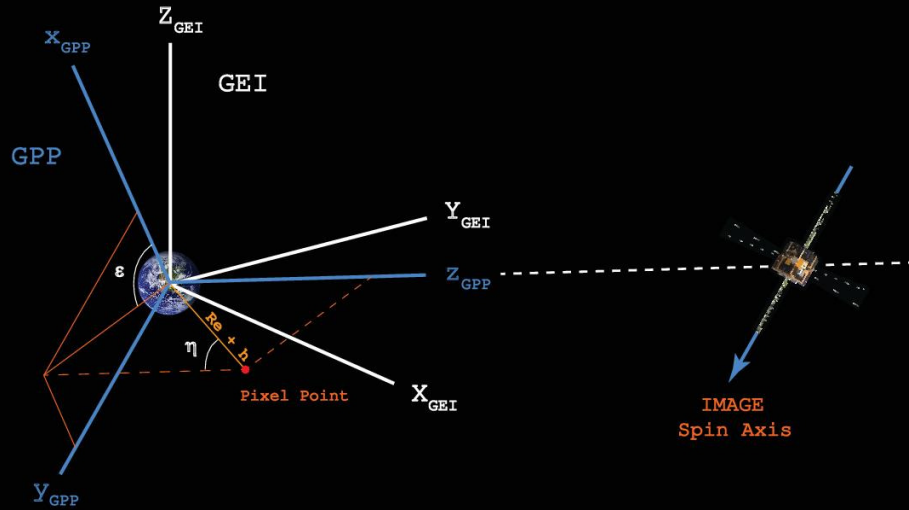
$$Pixel = [\sin\eta \cdot (R_e + h) \cos\varepsilon \quad \sin\eta \cdot (R_e + h) \sin\varepsilon \quad \cos\eta (R_e + h)]$$



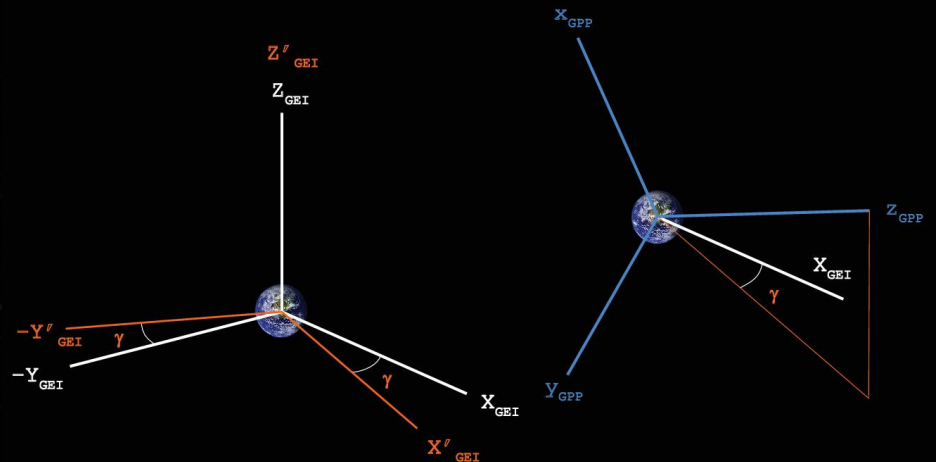
Data Analysis – Initial Points Collection



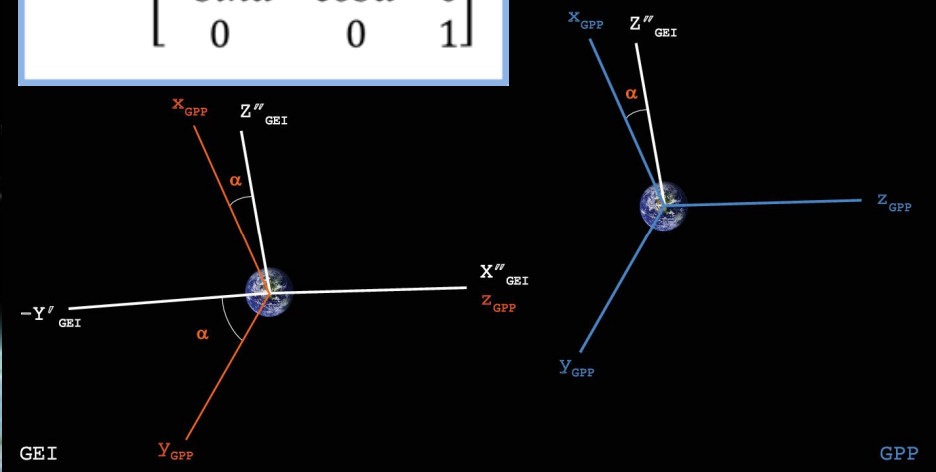
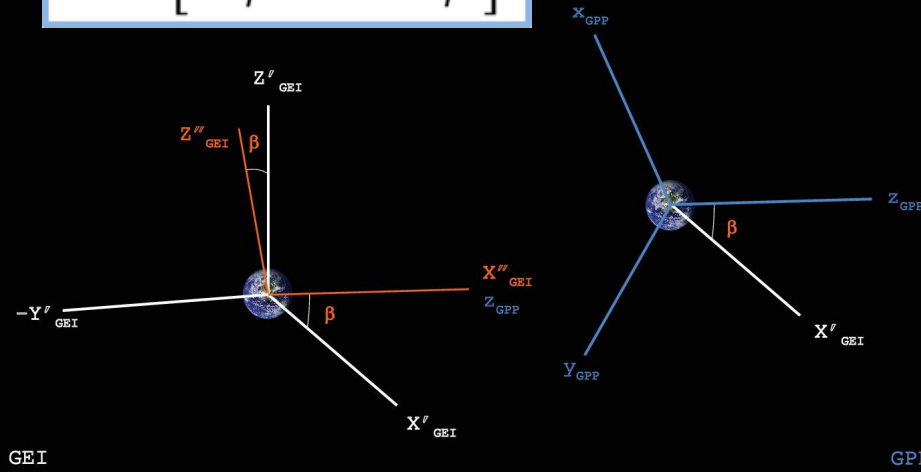
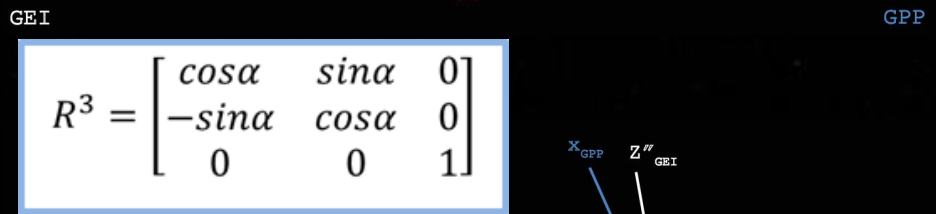
Rotation matrix



$$R^1 = \begin{bmatrix} \cos\gamma & \sin\gamma & 0 \\ -\sin\gamma & \cos\gamma & 0 \\ 0 & 0 & 1 \end{bmatrix}$$

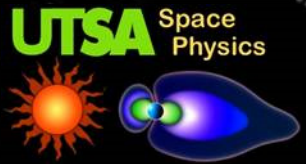


$$R^2 = \begin{bmatrix} \cos\beta & 0 & -\sin\beta \\ 0 & 1 & 0 \\ \sin\beta & 0 & \cos\beta \end{bmatrix}$$





Data Analysis – Post Processor



- Only consider points within $R_e + h$:

$$\lambda = \sin^{-1} \left(Z_{sm} / [R_e + h] \right)$$

$$L = (R_e + h) / \cos^2(\lambda)$$

$$\Lambda = \cos^{-1} \left(\sqrt{1/L} \right)$$

$$MLT = 12 + \left(\tan^{-1} \left(y_{sm} / x_{sm} \right) / \pi \right) \times 12$$

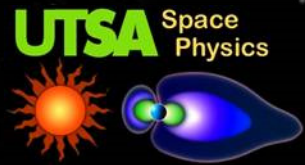
$$\alpha = \cos^{-1} \left[\frac{\vec{v}_{ena} \cdot \vec{B}}{|v_{ena}| |B|} \right]$$

- Final data: min/max/mean/median of valid points / pixel
- Fold Southern hemisphere into Northern

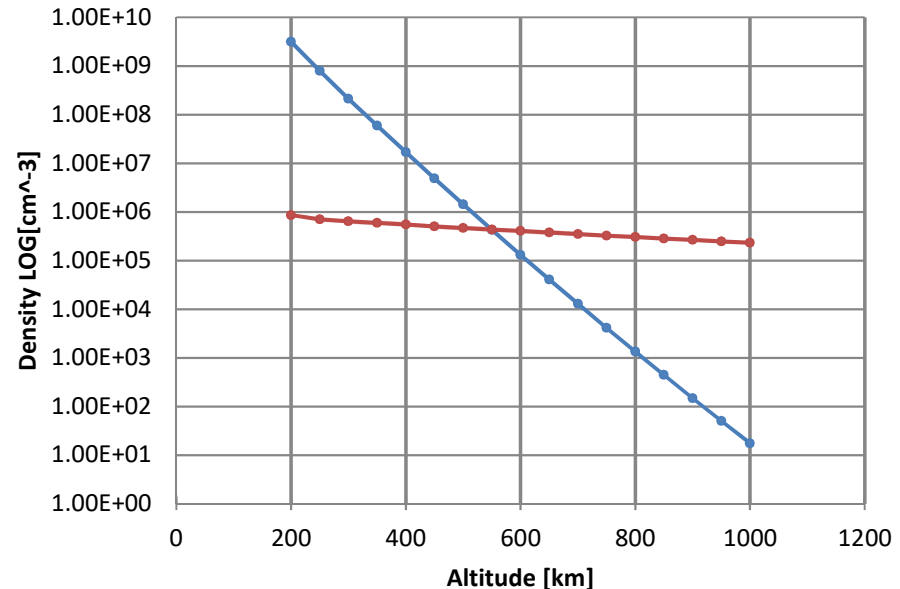




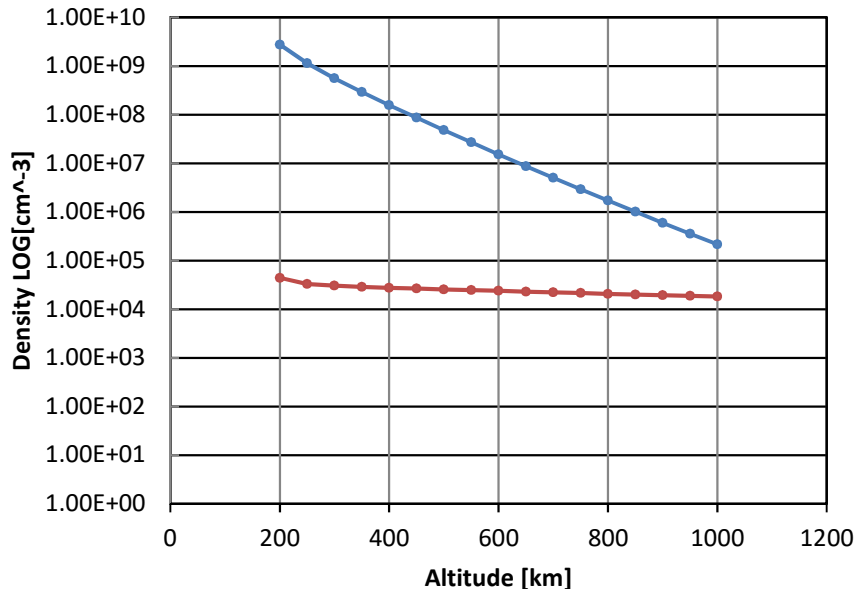
Short Aside: What is h in Re+h?



Solar Min (Jan 1 2007) F10.7=50



Solar Max (June 1 2000) F10.7=350

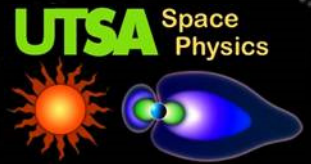


- Oxygen
- Hydrogen

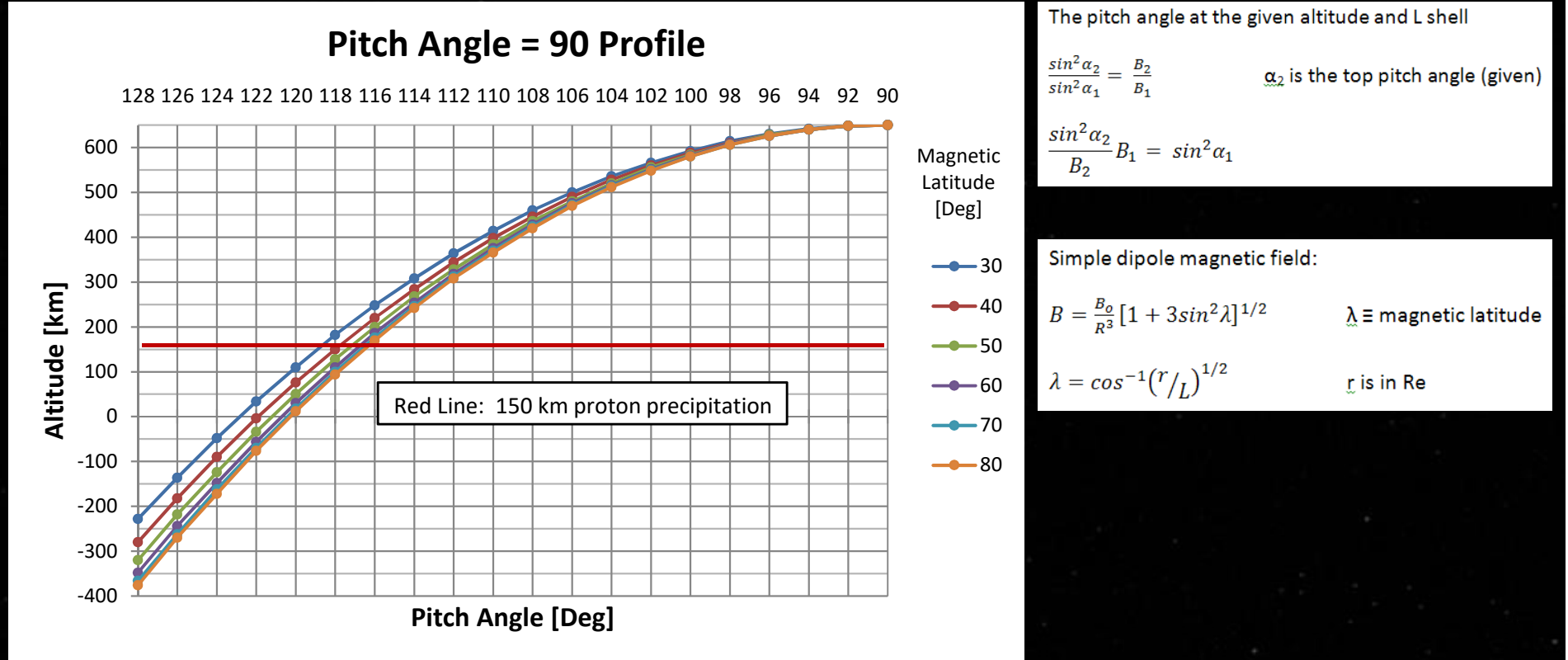




Data Analysis – Post Processor

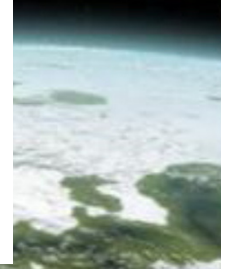


Only keep points that could have a mirror point above 150 km



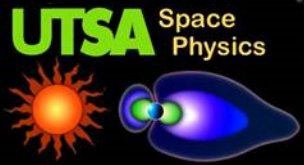
So given a λ , compute the L at 650 km. Follow the same L down to the mirror point

$$\sin^{-1} \left[\frac{\sin^2 \alpha_2}{(6370 + h)^3 [1 + 3\sin^2 \lambda]^{1/2}} (6370 + 650)^3 \left[1 + 3\sin^2 \left(\cos^{-1} \left[\frac{(R_e + h)}{R_e L} \right]^{1/2} \right) \right]^{1/2} \right]^{1/2} = \alpha_1$$





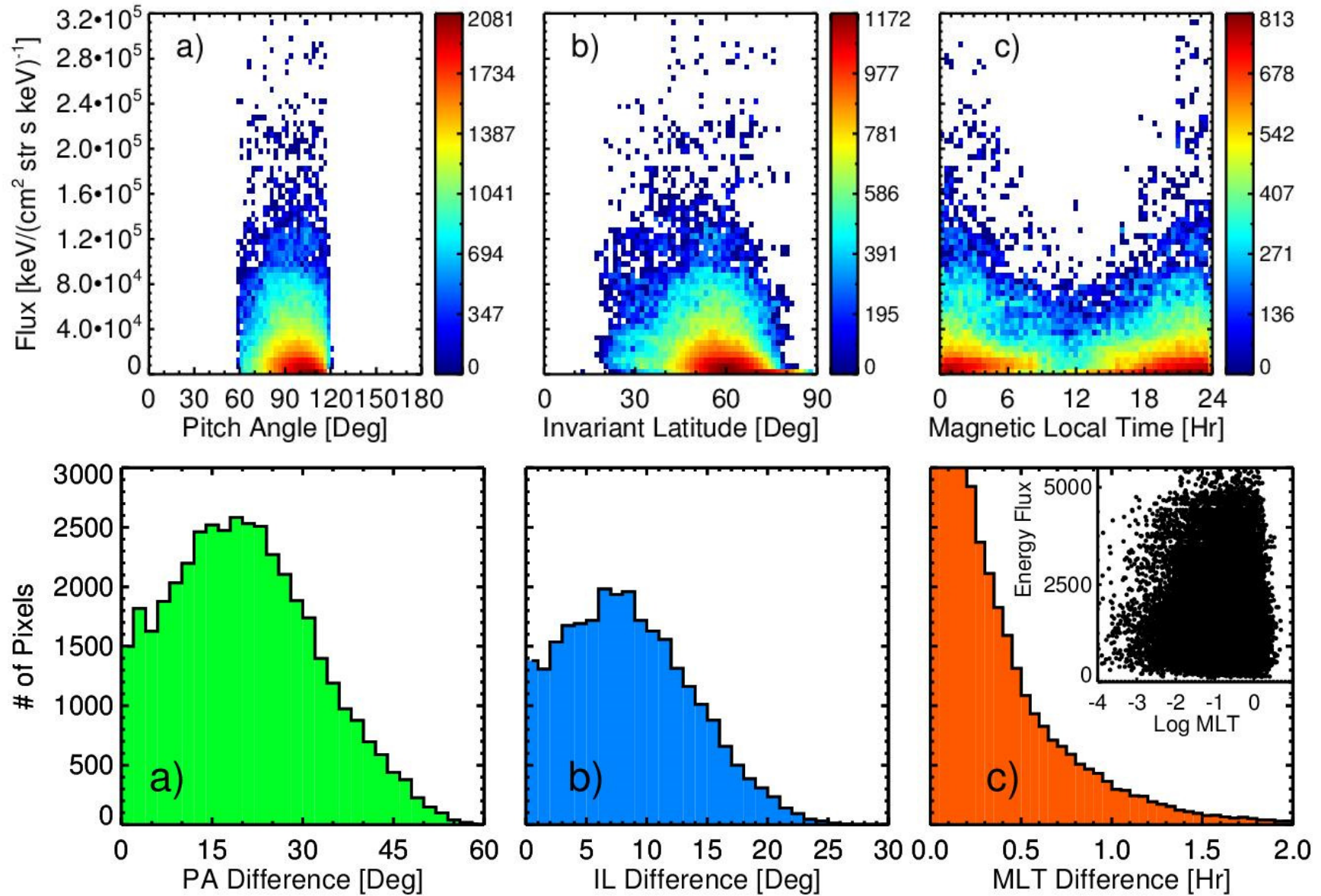
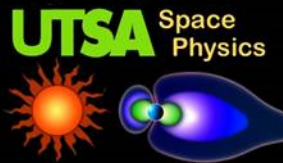
Outline of Topics



- Objective / Merits of the Study
- Introduction
- Data Analysis
- Results
 - LAE Geomagnetic Index Correlation
 - LAE/In Situ Response to Storms
 - LAE/In Situ Correlation
 - LAE/In Situ Comparison

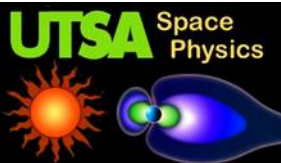


All LAE Pixels 2000 - 2005

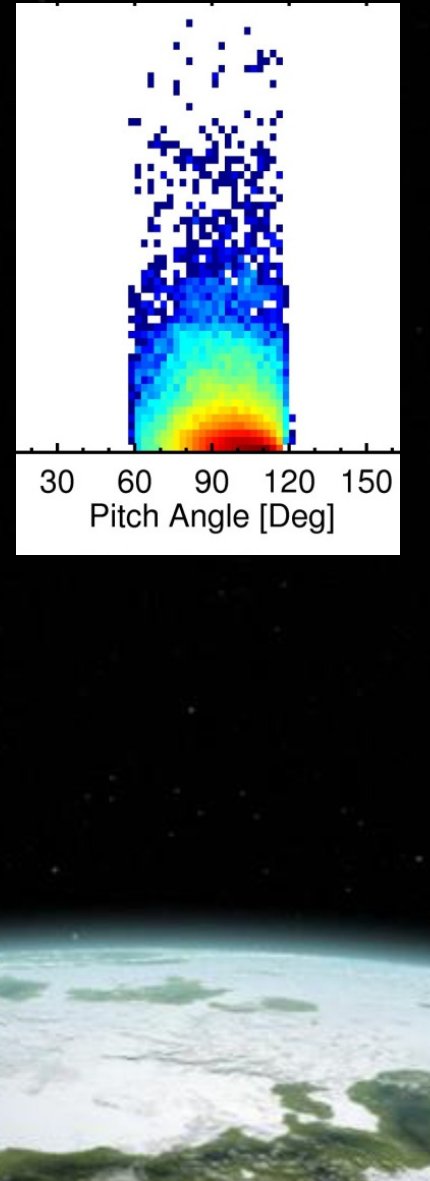
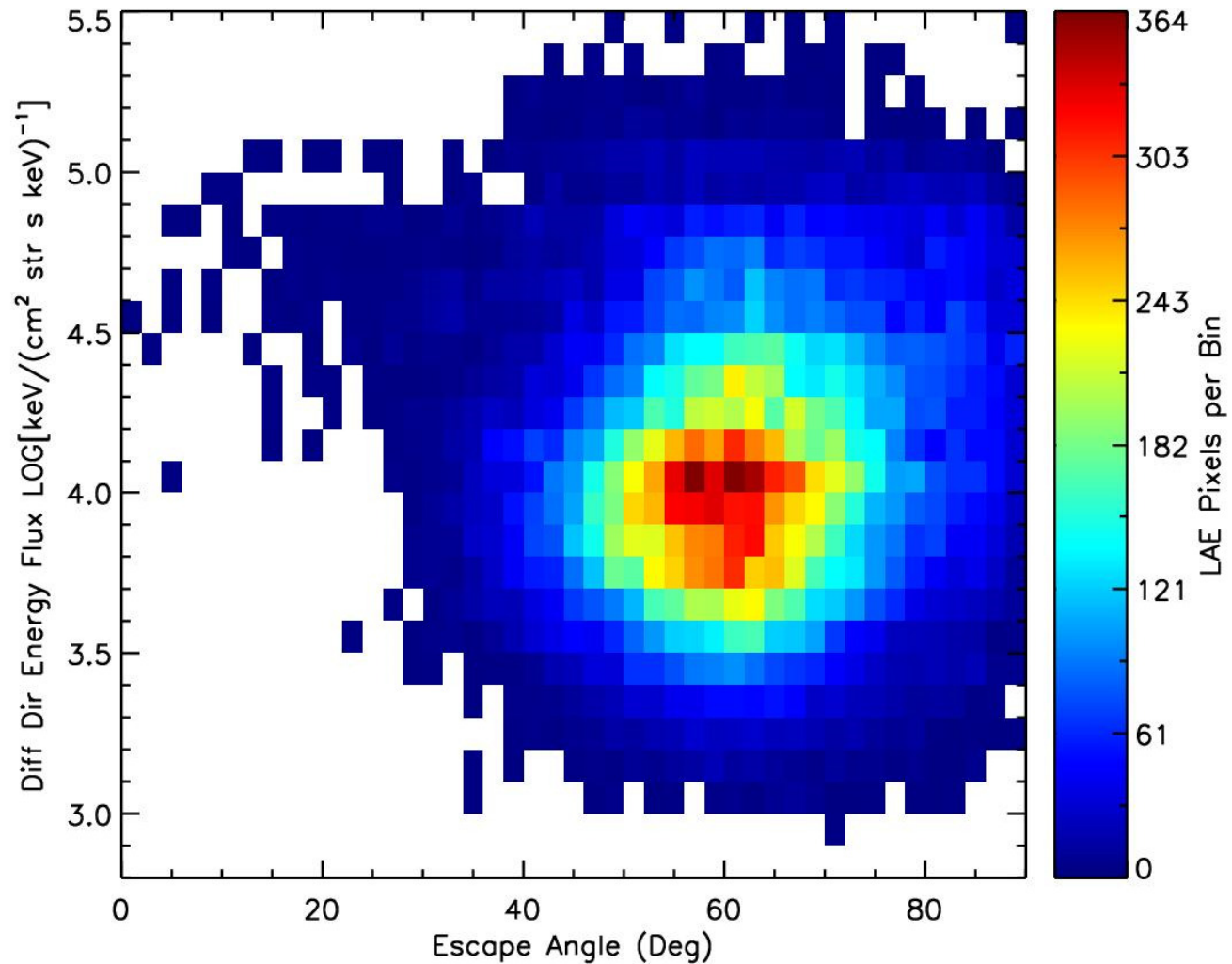




All LAE Pixels 2000 - 2005

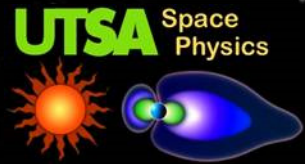


Escape Angle





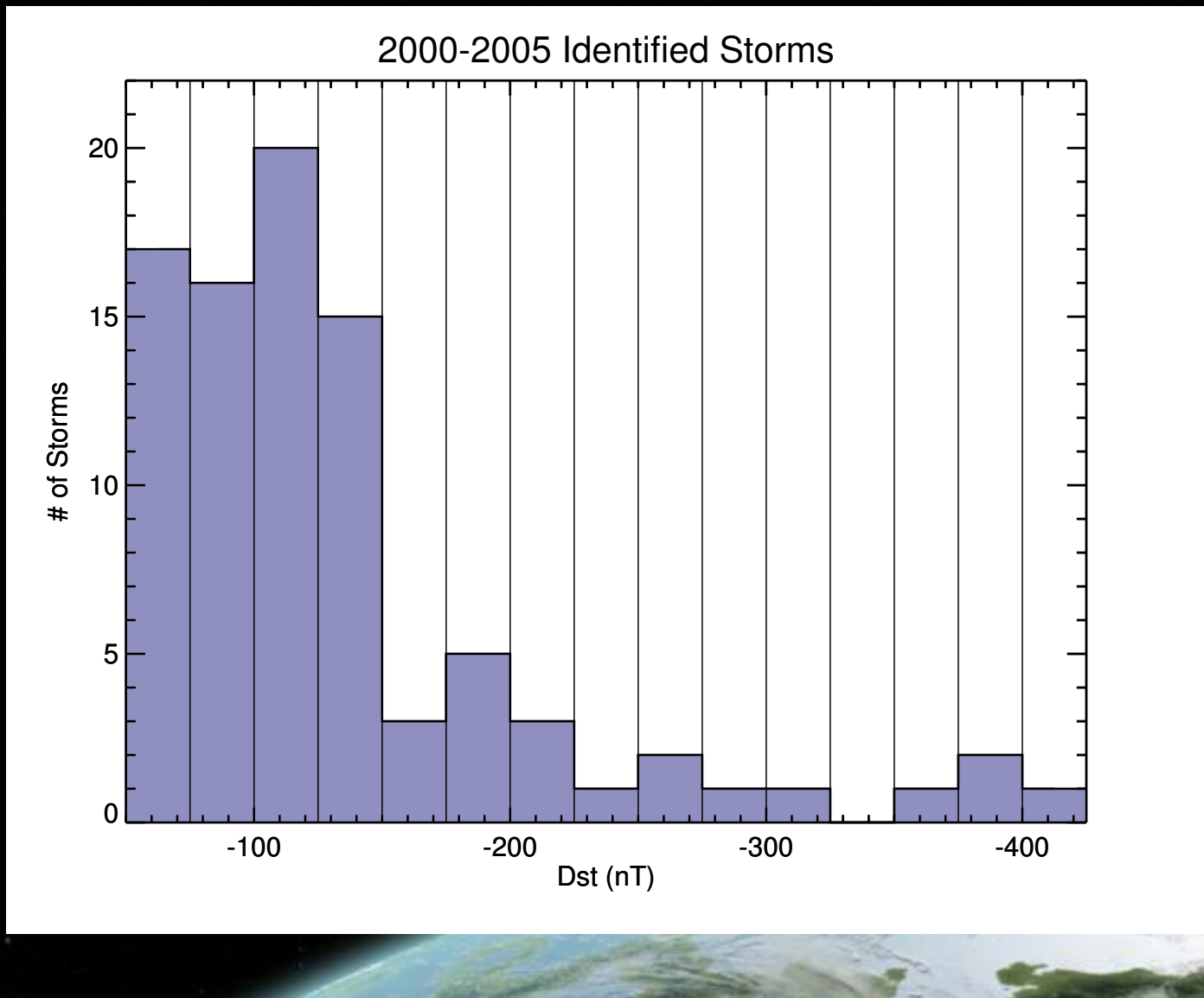
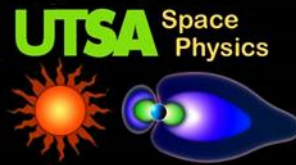
Outline of Topics



- Objective / Merits of the Study
- Introduction
- Data Analysis
- Results
 - LAE Geomagnetic Index Correlation
 - LAE/In Situ Response to Storms
 - LAE/In Situ Correlation
 - LAE/In Situ Comparison

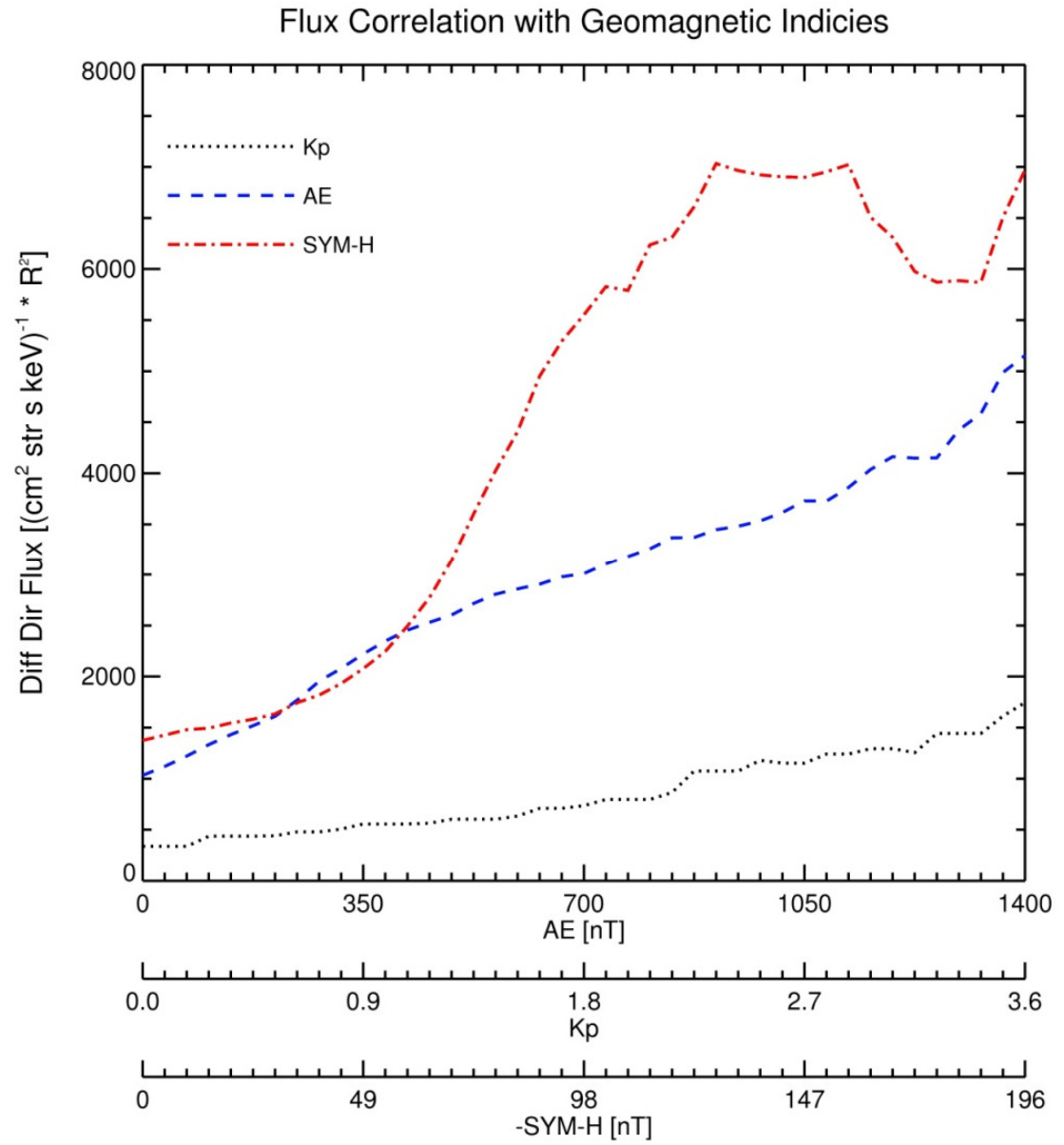
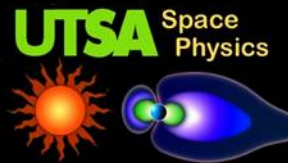


Quick Aside - Storm List



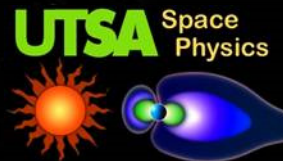


Flux Trendline





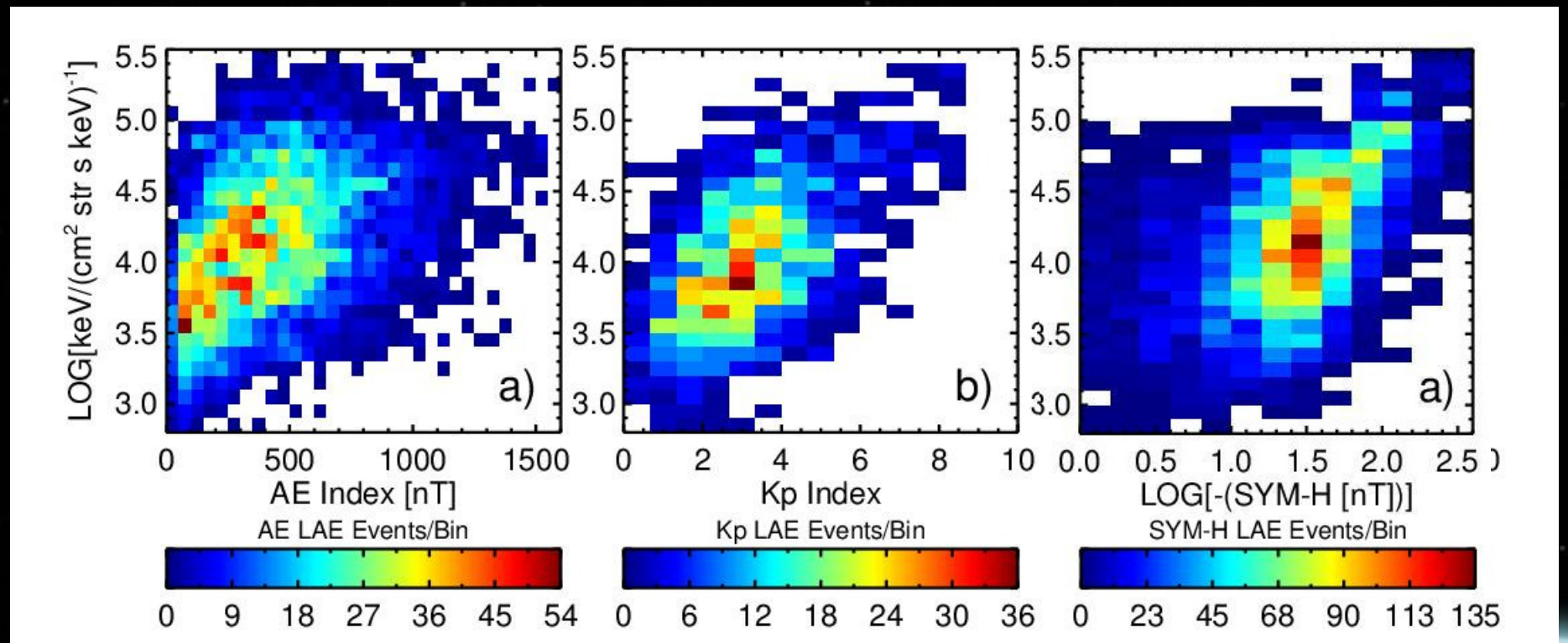
Flux Correlation



PCC: **0.388 [15%]**

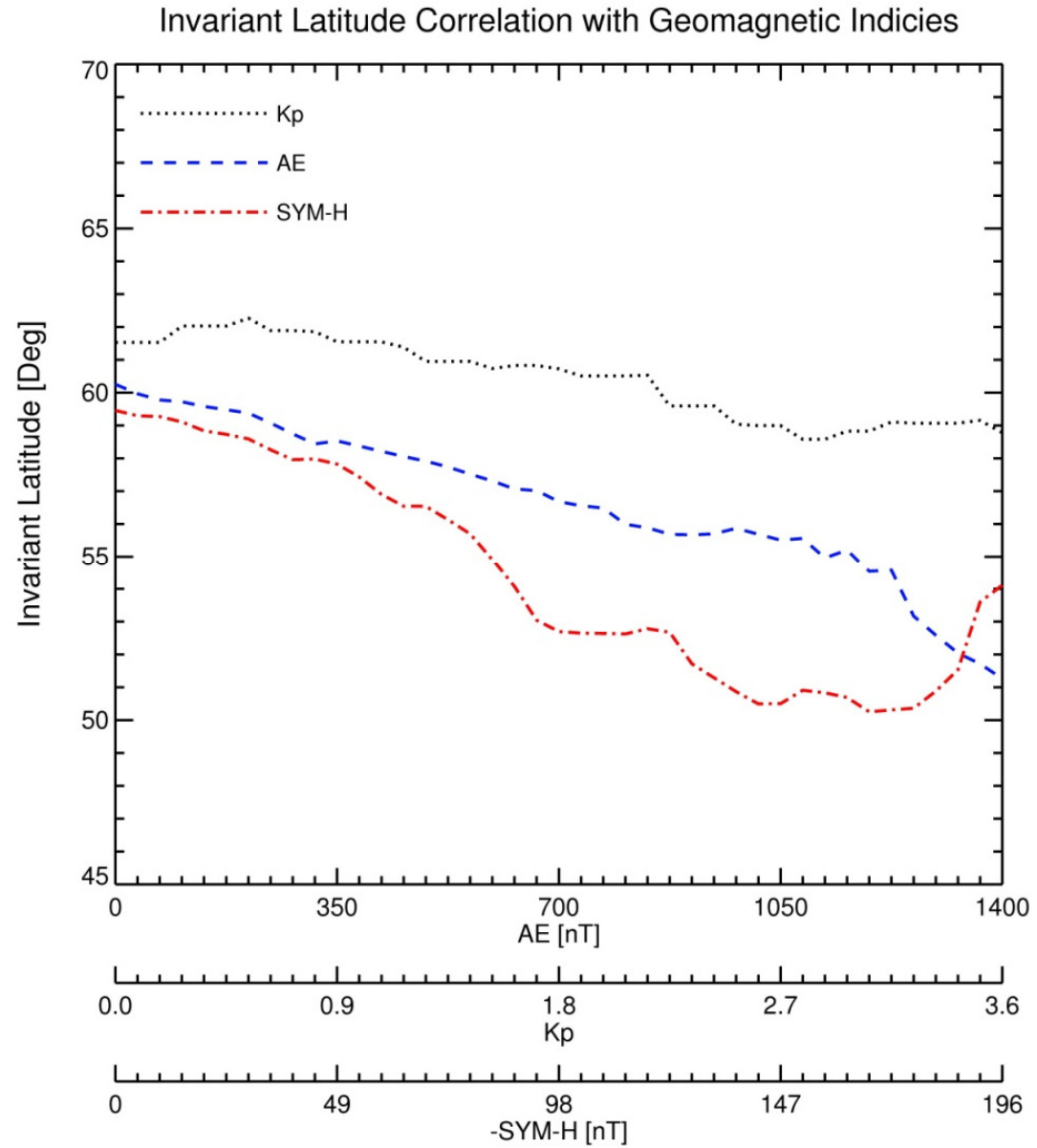
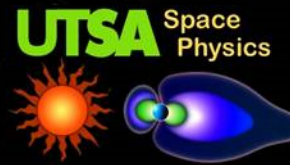
0.564 [32%]

0.531 [28%]



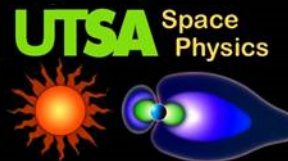


Invariant Latitude Trendline





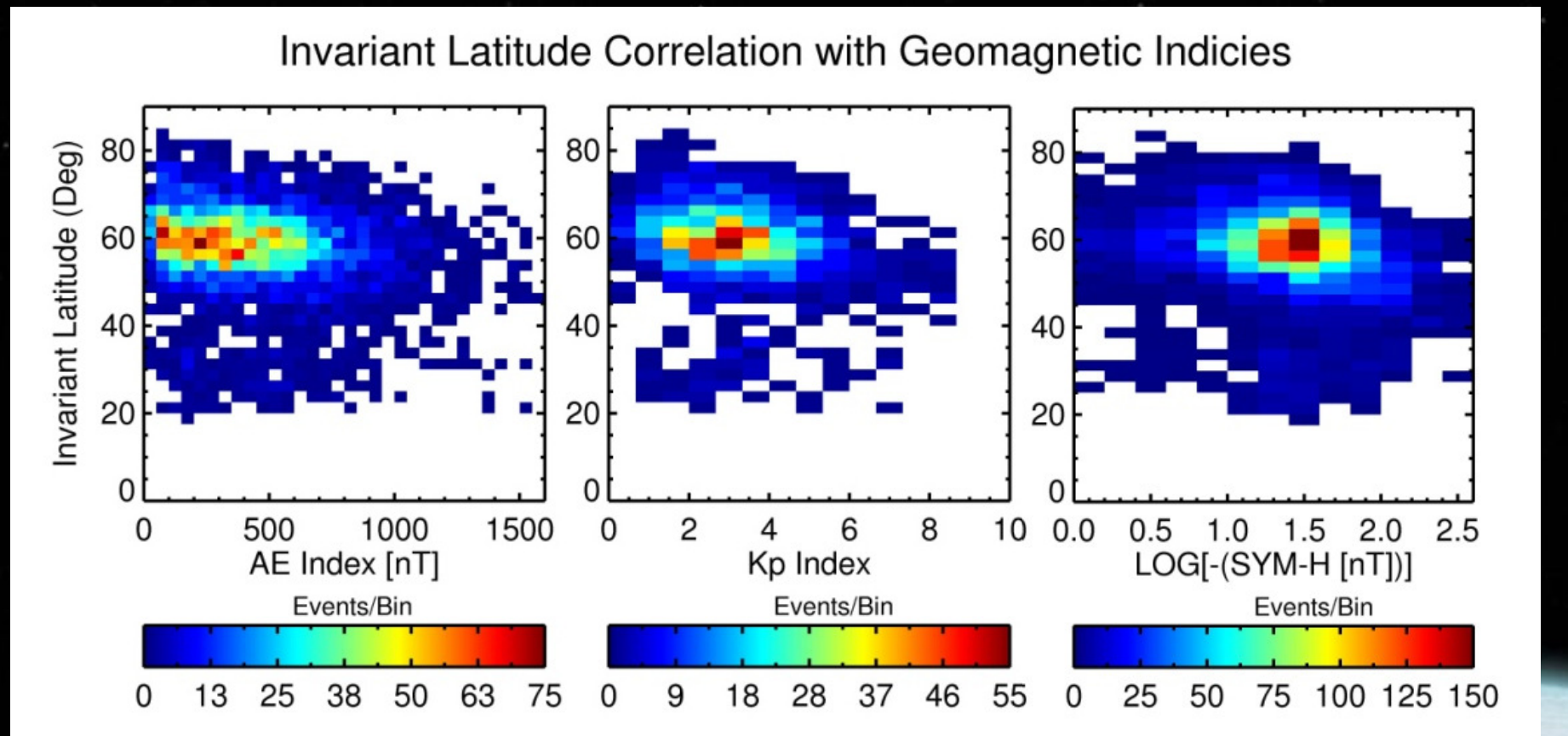
Invariant Latitude Correlation



PCC: -0.186 [3.5%]

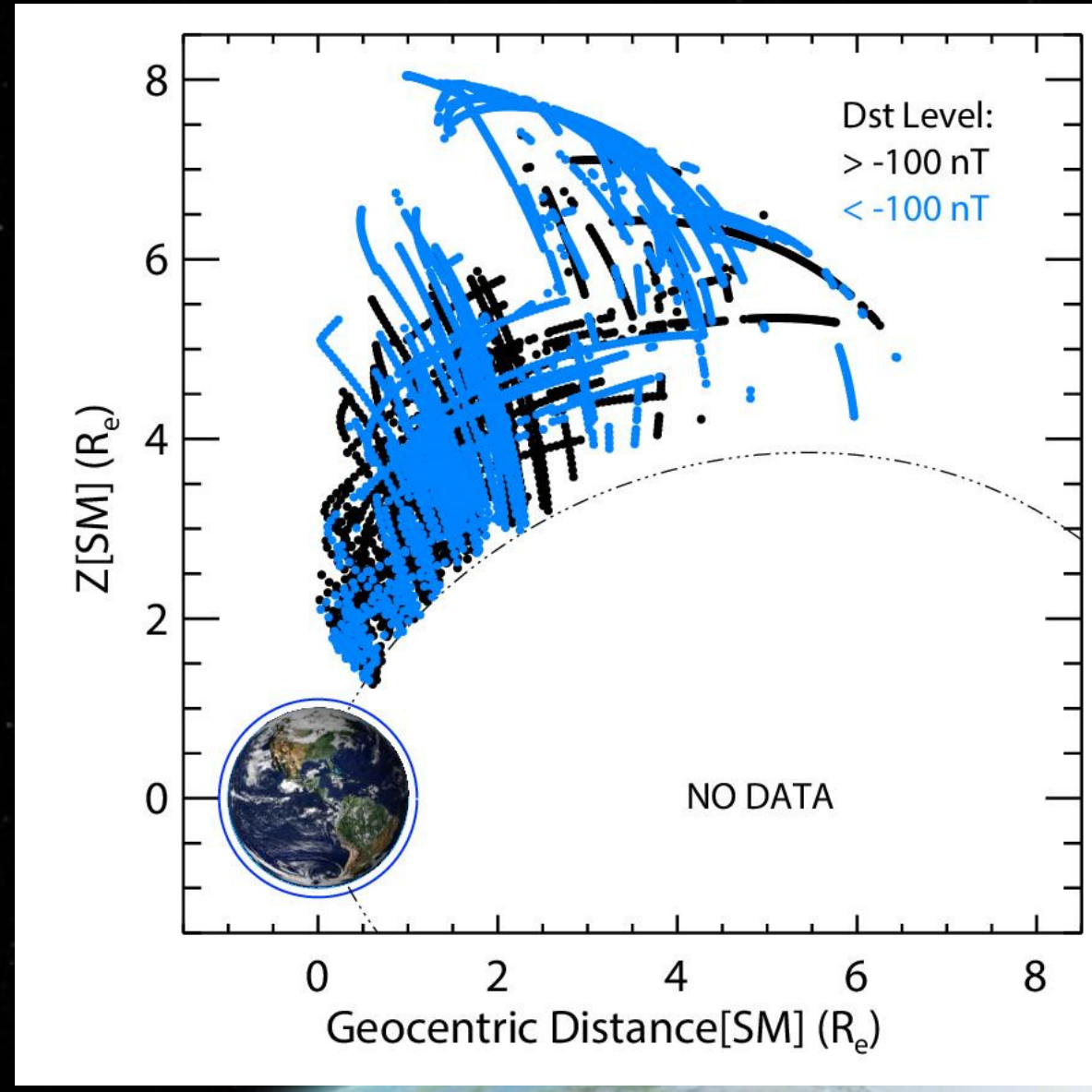
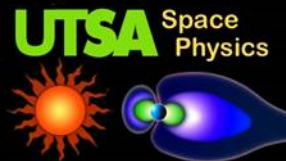
-0.207 [4.3%]

-0.209 [4.4%]



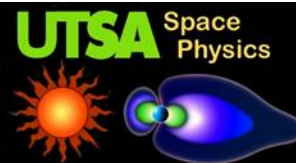


Invariant Latitude Sampling - Bias?

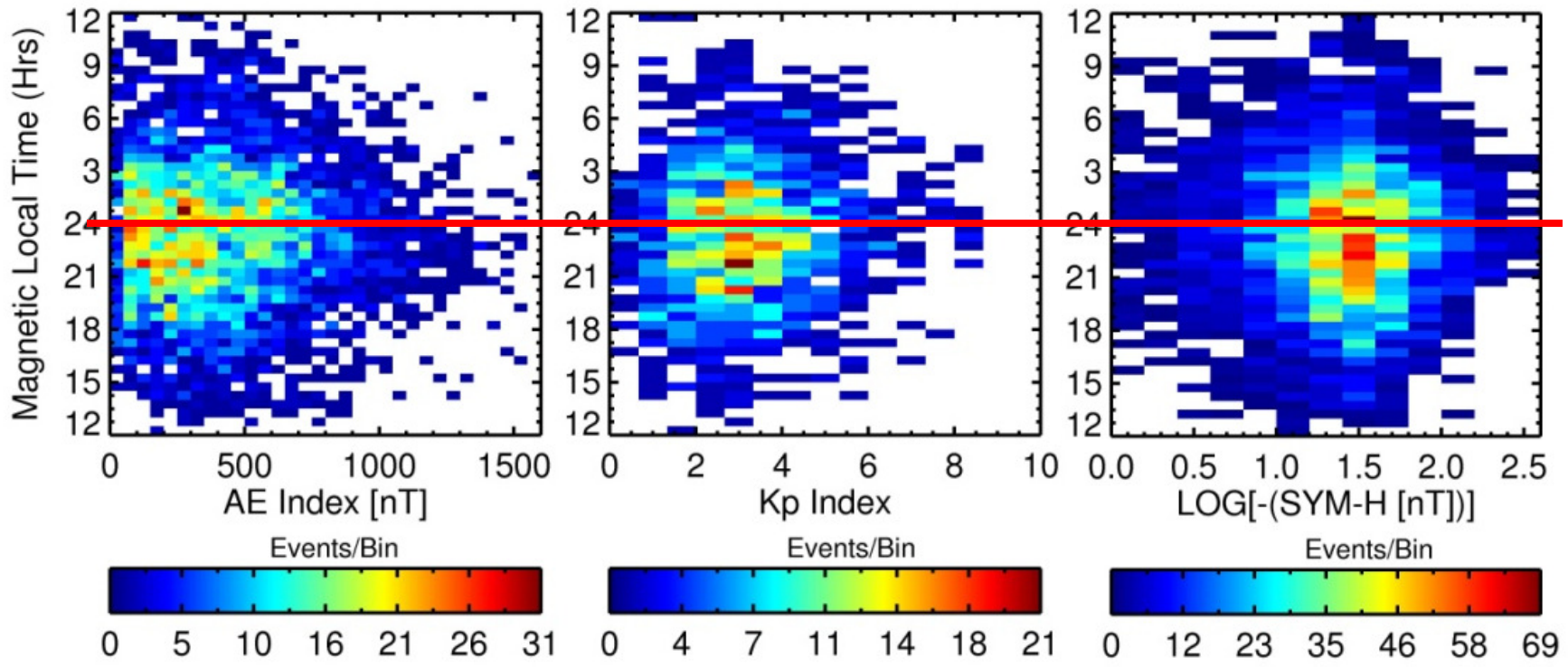




Magnetic Local Time Correlation

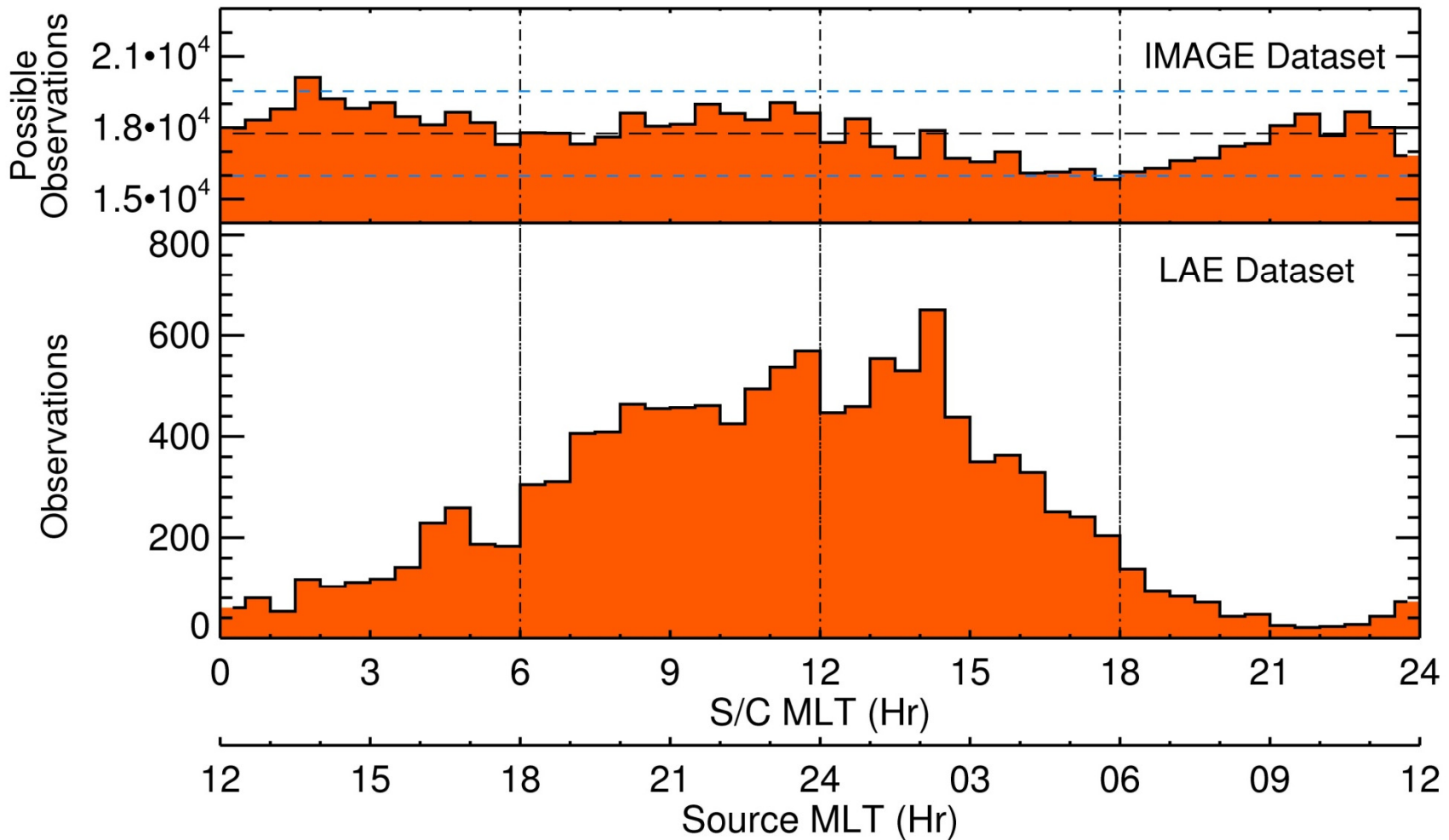
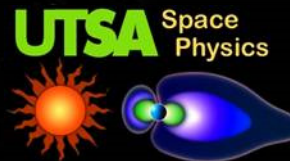


Magnetic Local Time Correlation with Geomagnetic Indicies



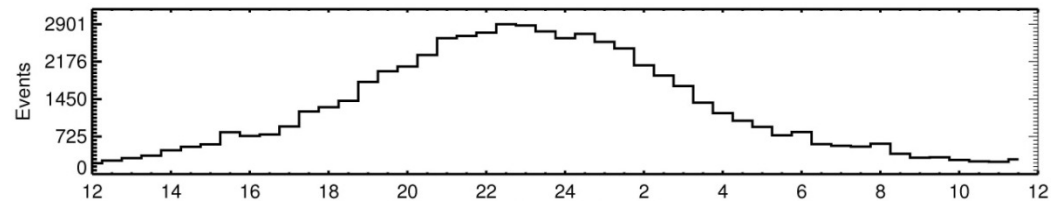
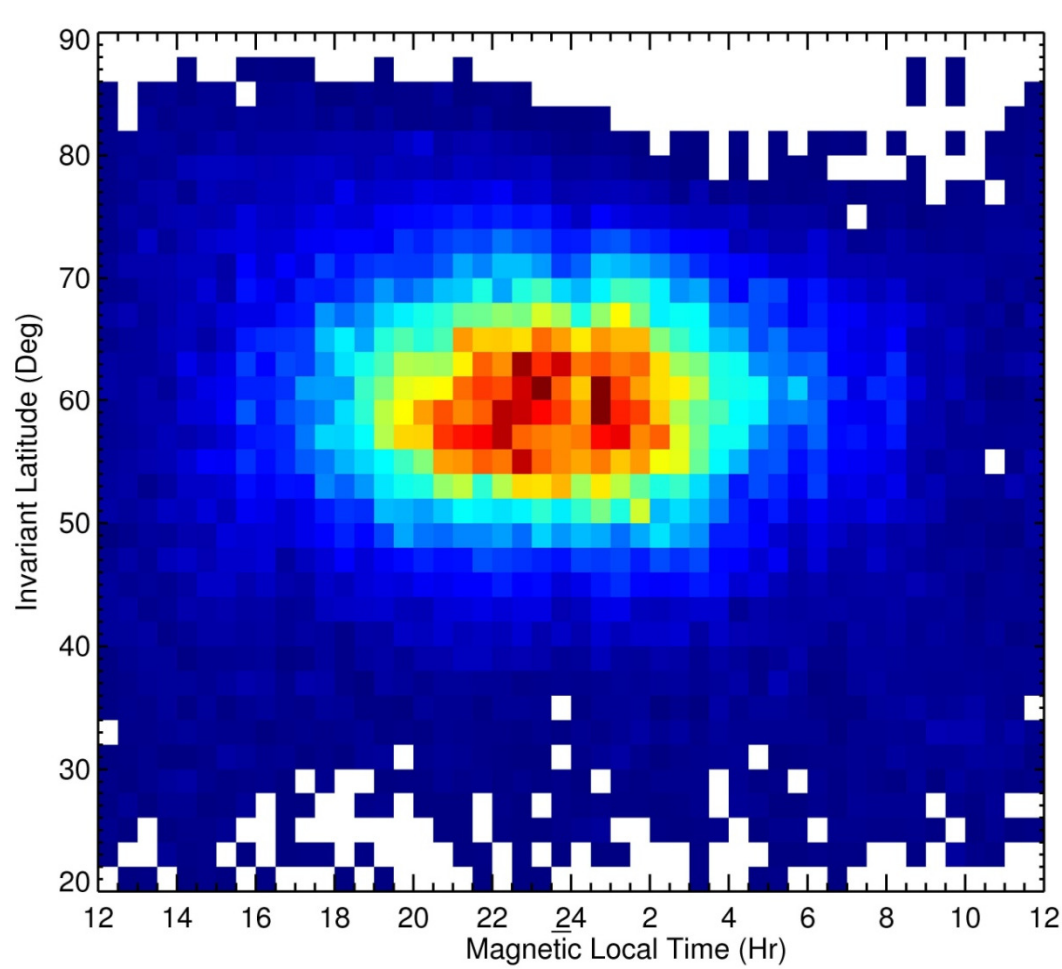
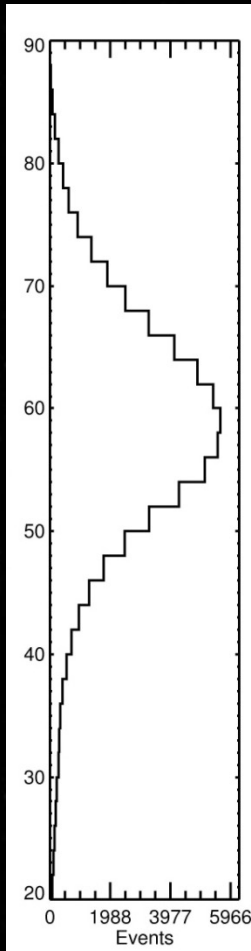
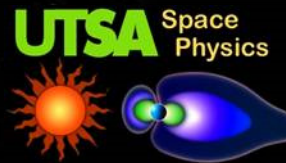


MLT Sampling - Bias?



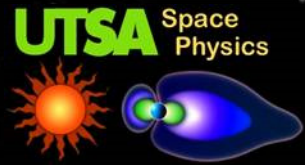


MLT / IL Correlation





Outline of Topics

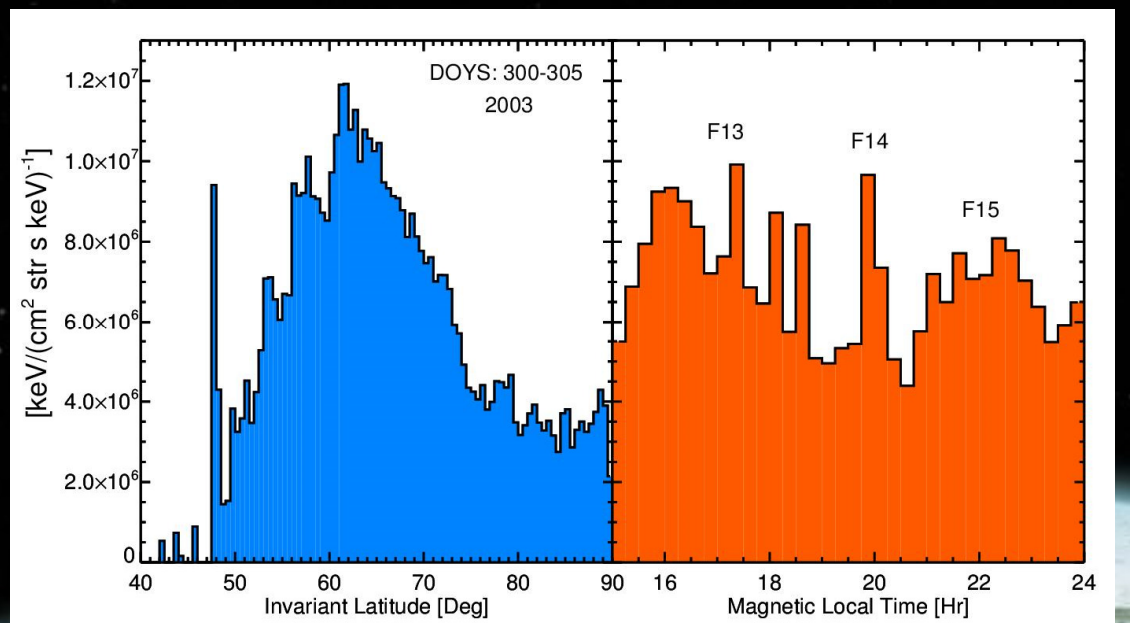
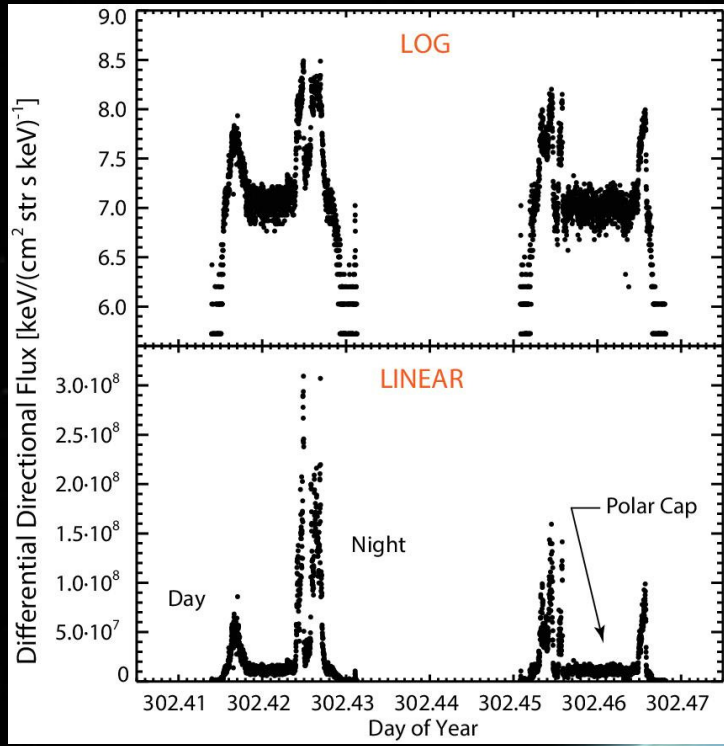
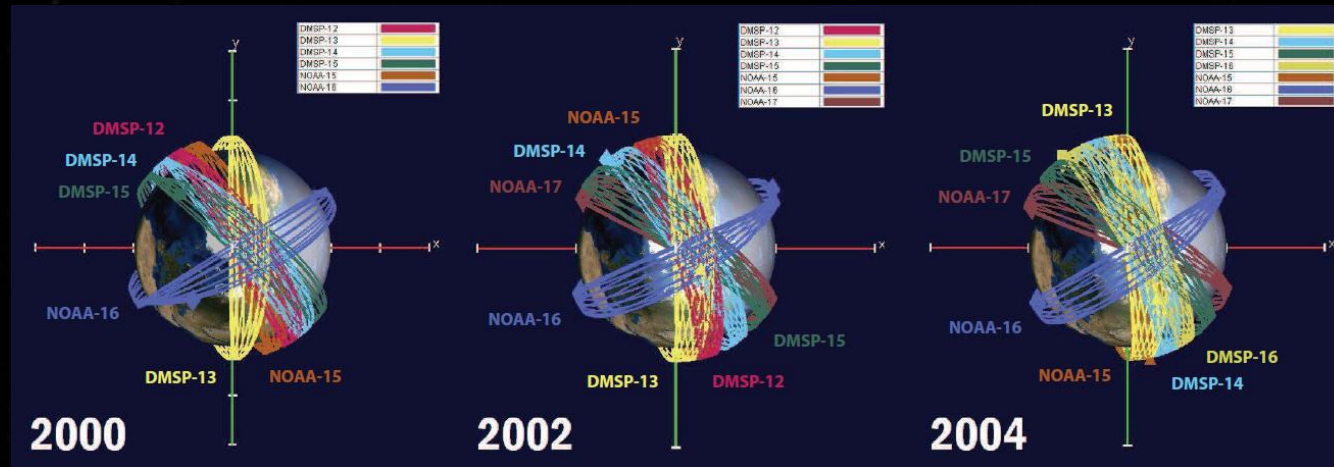
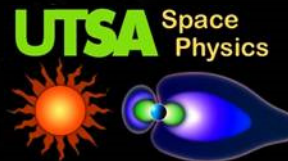


- Objective / Merits of the Study
- Introduction
- Data Analysis
- Results
 - LAE Geomagnetic Index Correlation
 - LAE/**In Situ** Response to Storms
 - LAE/**In Situ** Correlation
 - LAE/**In Situ** Comparison



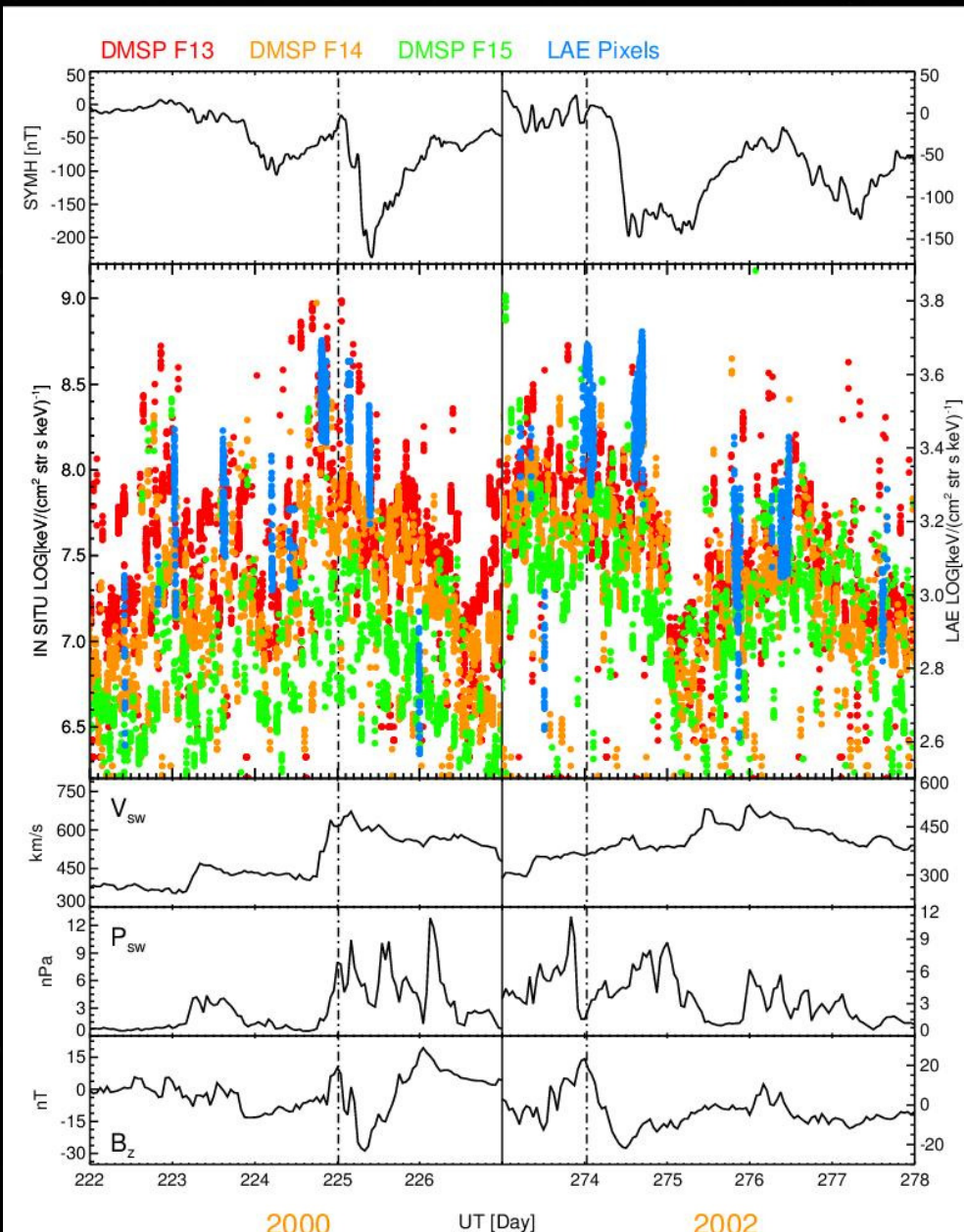
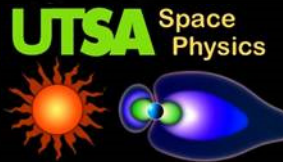
In-Situ Ion Data

Source: DMSP SSJ/4 2000-2005



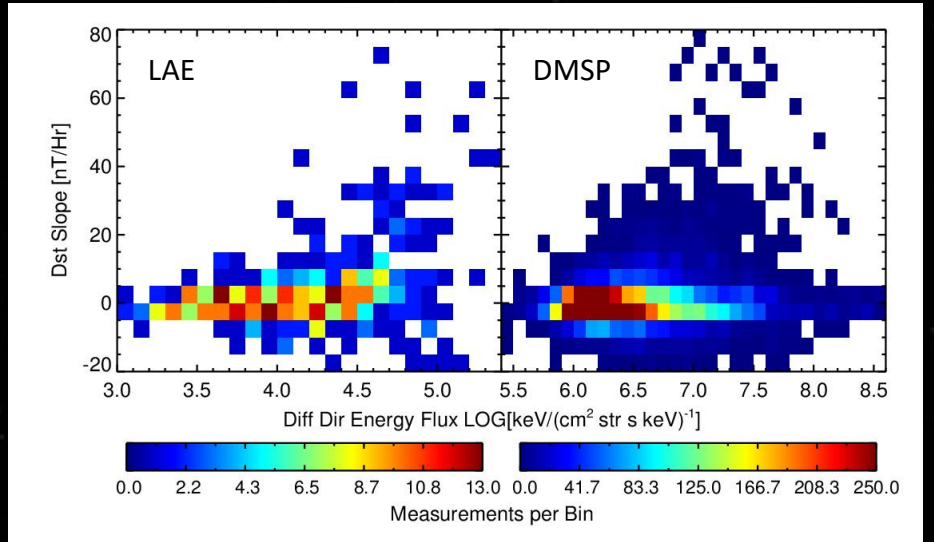
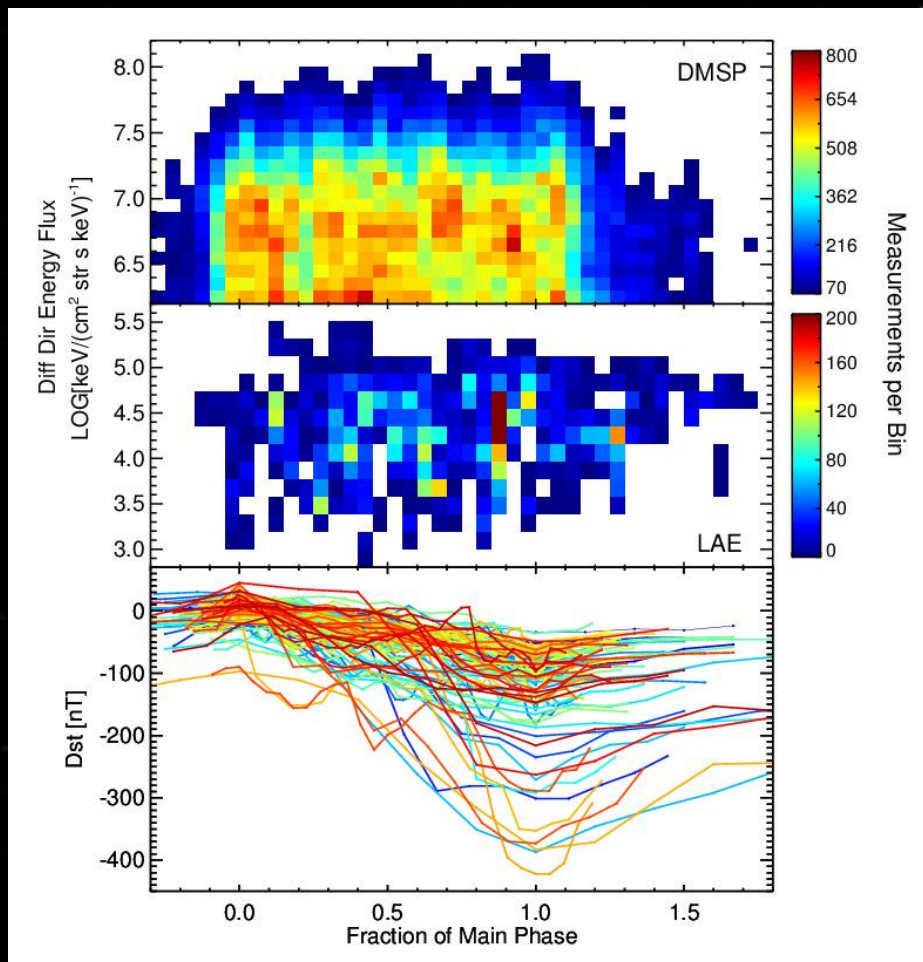
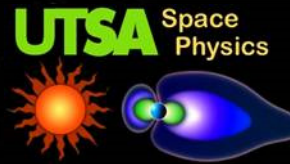


Sample Storm Response



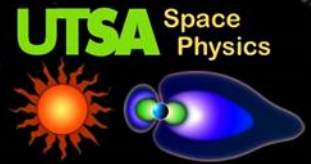


Sample Storm Response



- **Geomagnetic Parameters:**
 - Dst [SYM-H] Magnitude
 - Slope

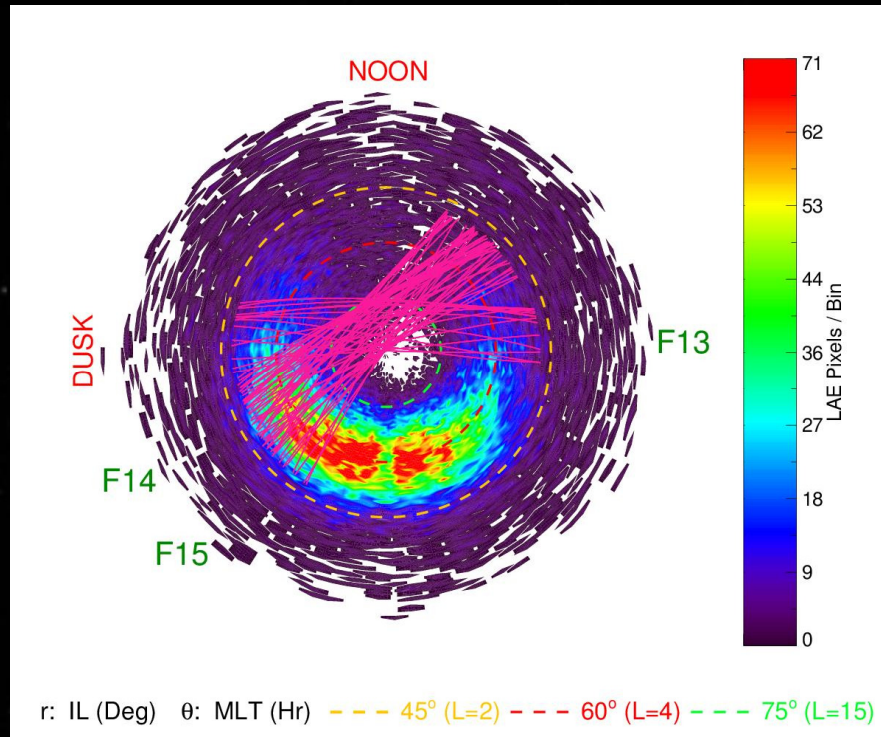
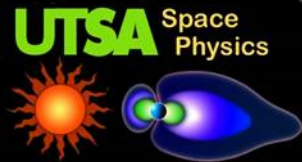




- Objective / Merits of the Study
- Introduction
- Data Analysis
- Results
 - LAE Geomagnetic Index Correlation
 - LAE/In Situ Response to Storms
 - LAE/In Situ Correlation
 - LAE/In Situ Comparison

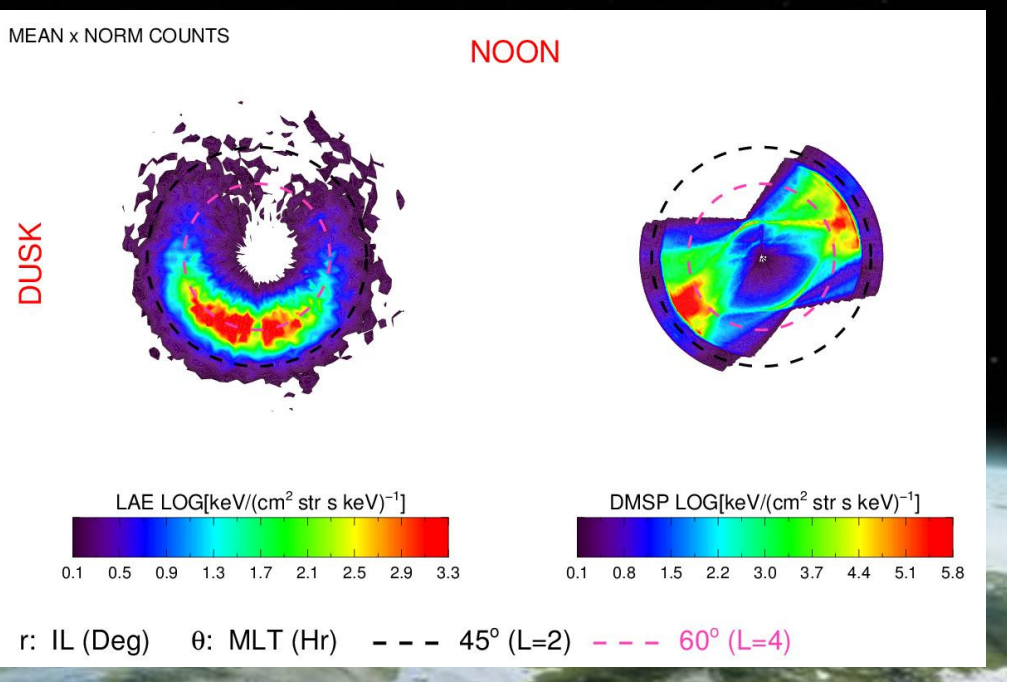


LAE / In Situ Correlation



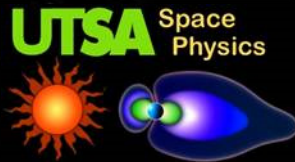
Magenta: DMSP passes

- Bin size
 - IL: 0.7°
 - MLT: 0.25 Hr





Flux – Flux Correlation



Binned +/- 1 min
to LAE pixel

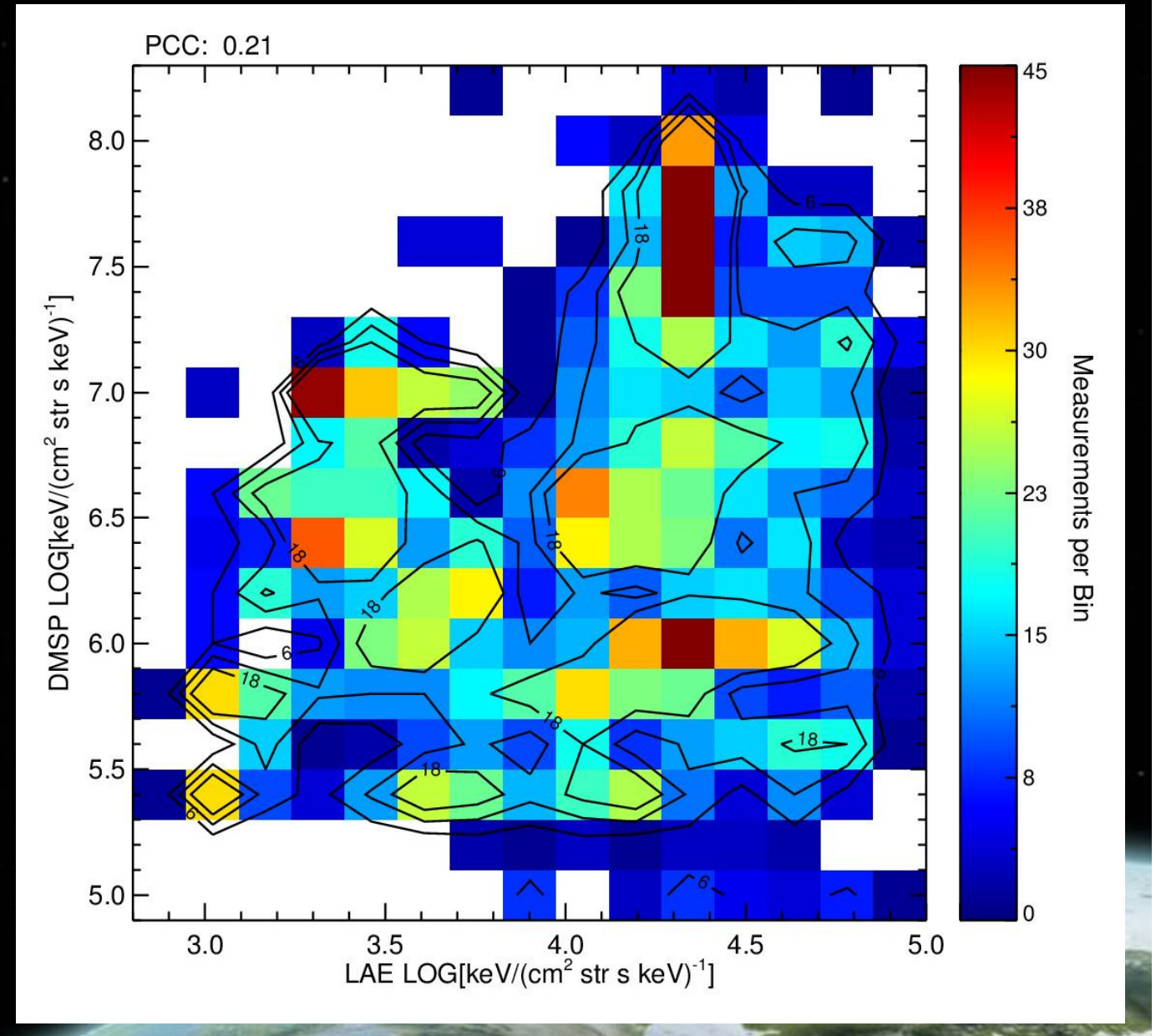
Flux Bin Size

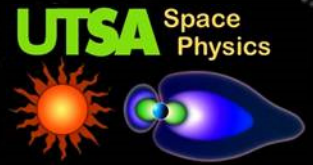
- LAE: 1.5
- DMSP: 2.0

Contours [6, 12, 18]

Not well correlated

- 4.4% of variability
is related



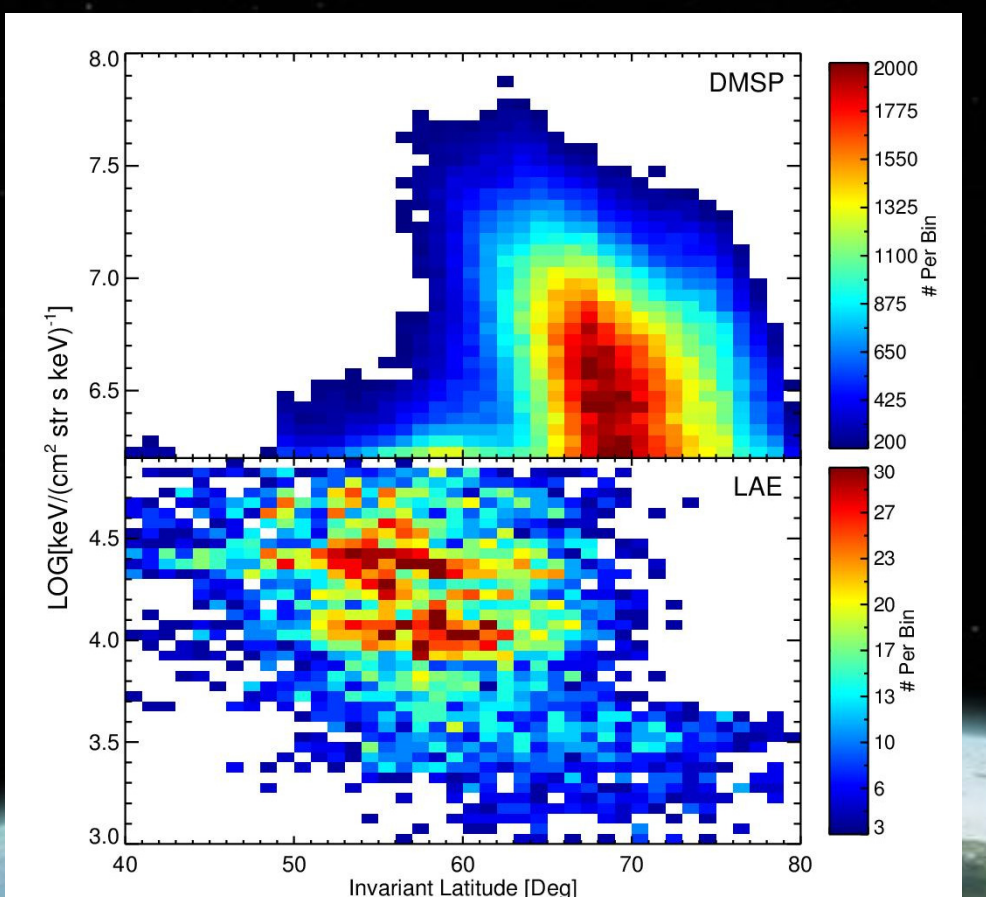
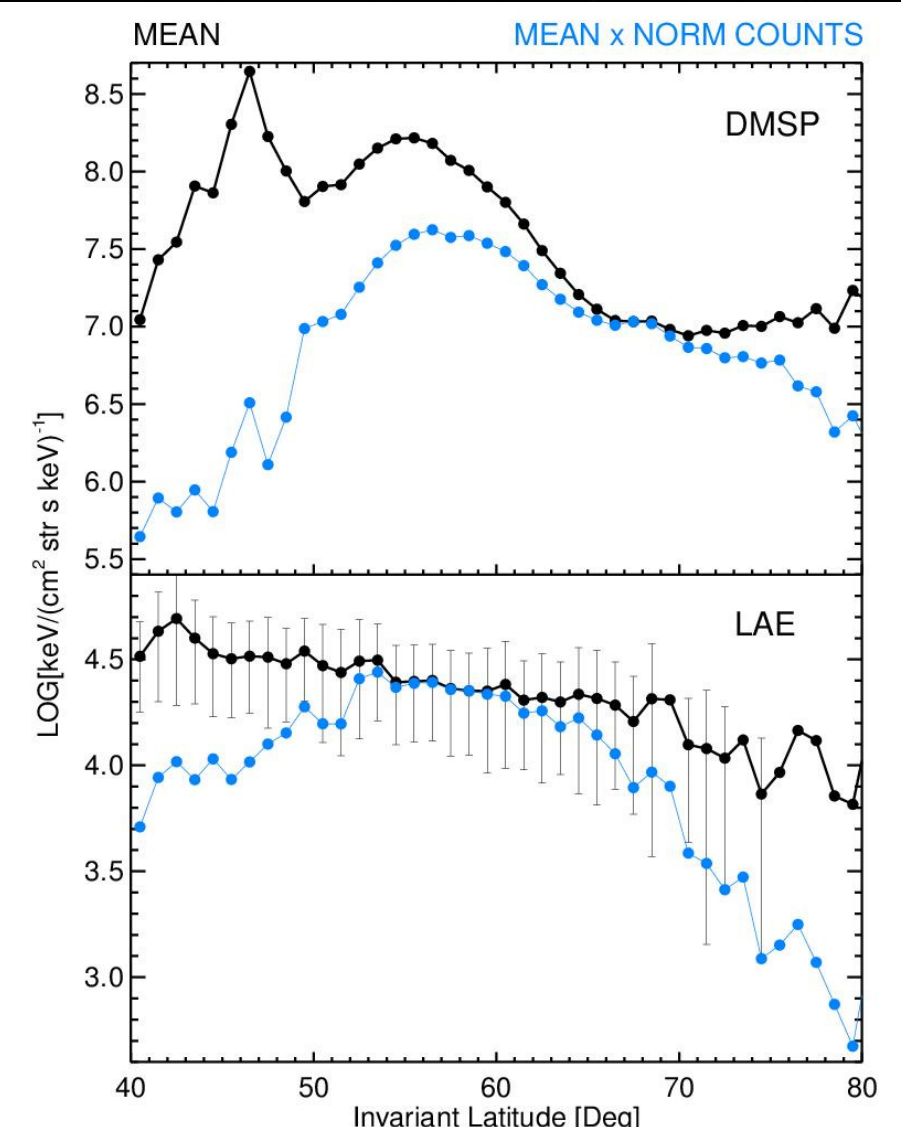
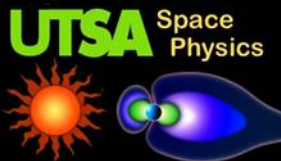


- Objective / Merits of the Study
- Introduction
- Data Analysis
- Results
 - LAE Geomagnetic Index Correlation
 - LAE/In Situ Response to Storms
 - LAE/In Situ Correlation
 - LAE/In Situ Comparison



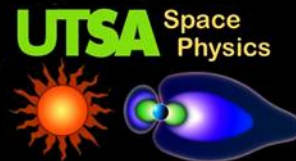


Diff Dir Energy Flux as a Function of IL

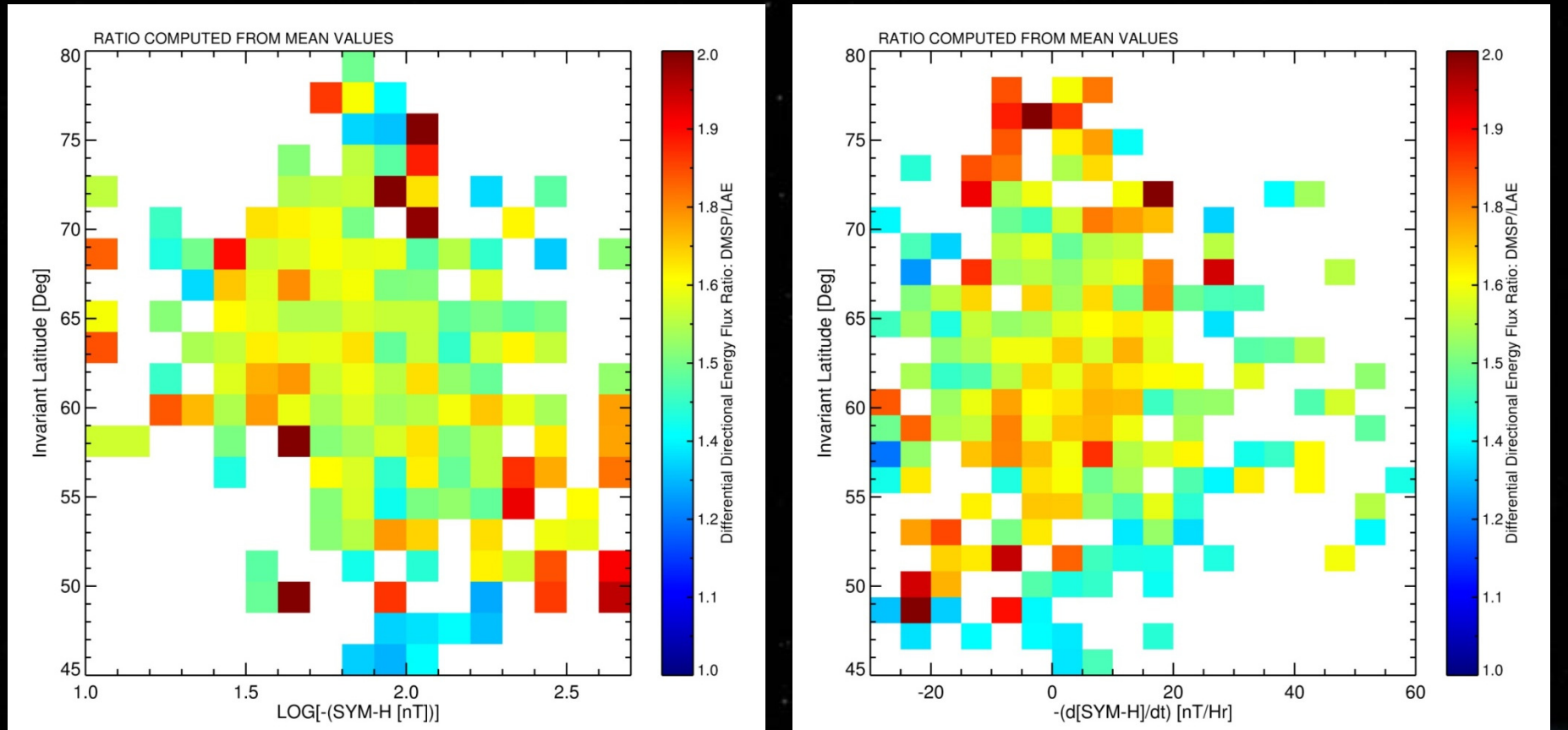




LAE / In Situ Comparisons



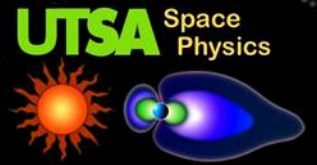
Ratio of the LOG Diff Dir Energy Flux





Correlation Study Conclusions

LAE Geomagnetic Correlation



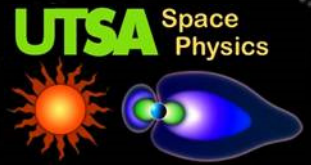
- Response of LAE flux to SYM-H is the most sensitive (rapid change)
- The Invariant Latitude of LAEs decreases (lower L-Shell) with increasing geomagnetic activity
- NOT ring current particles (too low in energy) – BUT shows an association with ring current activity
- Plasma population is most consistent to what is observed from the plasma sheet
- Invariant latitude uncertainty is not too large

Can be used for storm time studies to access ion precipitation



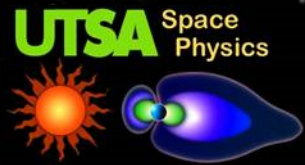
Correlation Study Conclusions

LAE DMSP Comparison



- DMSP orbit is too limited to evaluate large scale MLT dependence in flux
- Both LAE and DMSP respond similarly to geomagnetic activity, immediately increasing after beginning of main phase and ceasing shortly after end of main phase
- No Flux-Flux correlation evident
 - Spatial restrictions, Different physical processes
- IL distributions differ
 - LAE is more spread out and slightly lower
- Ratio of flux is fairly constant over geomagnetic activity
 - Possible exception of LAEs favored at higher flux, lower latitude
 - IL differences also evident in ratio



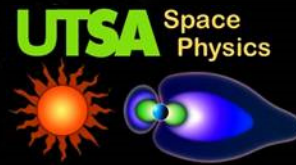


Thank You



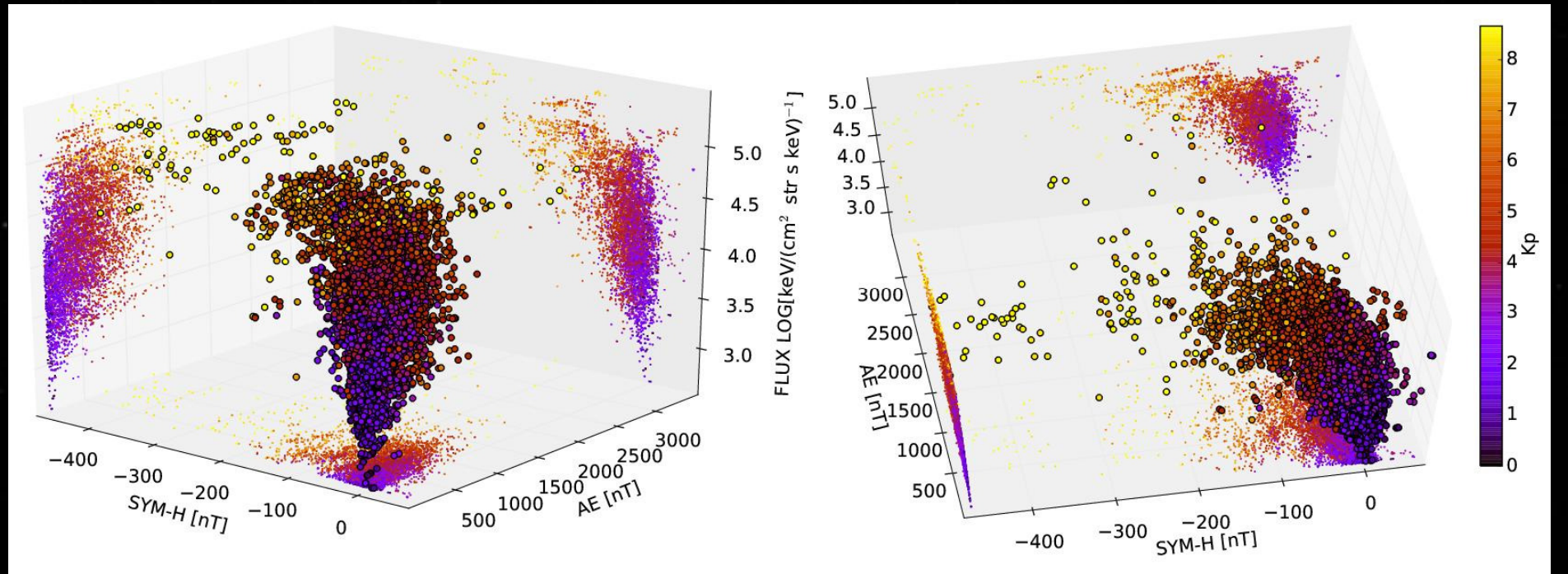


Extra Slides





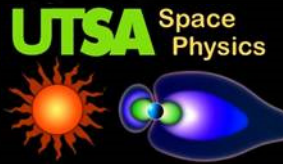
Multivariate Correlation



Multivariant Correlation Coefficient: 0.584 [34%]



Altitude Systematic Error



az_sample: 6°

el_sample: 7.5°

$\sigma = 9.6^\circ$

$$\eta = [\pi - \text{sigma}] - \left[\pi - \sin^{-1} \left(\frac{R \cdot \sin [\text{sigma}]}{R_e + h} \right) \right]$$

$$\varepsilon = \tan^{-1} (az_sample / el_sample)$$

$$Pixel = [\sin \eta \cdot (R_e + h) \cos \varepsilon \quad \sin \eta \cdot (R_e + h) \sin \varepsilon \quad \cos \eta (R_e + h)]$$

$h_1 = 400$ km % Diff in r: 4.4%

$h_2 = 700$ km At 5 R_e (dist. corr.): 4.2%

$r_1 = 6771$ km (1.03 R_e)

$\lambda_1 = 45.93^\circ$

$r_2 = 7071$ km (1.11 R_e)

$\lambda_2 = 50.78^\circ$

$\eta_1 = 44.45^\circ$

$L_1 = 2.13$

$\eta_2 = 39.10^\circ$

$L_2 = 2.78$

$\varepsilon_{1,2} = 38.66$

$$\lambda = \sin^{-1} \left(Z_{sm} / [R_e + h] \right)$$

$\text{Pixel}_1 = [0.56 \quad 0.45 \quad 0.74]$

$\text{Pixel}_2 = [0.55 \quad 0.44 \quad 0.86]$

$$L = (R_e + h) / \cos^2(\lambda)$$

$$\Lambda = \cos^{-1} \left(\sqrt{1/L} \right)$$

$IL_1 = 46.75^\circ$

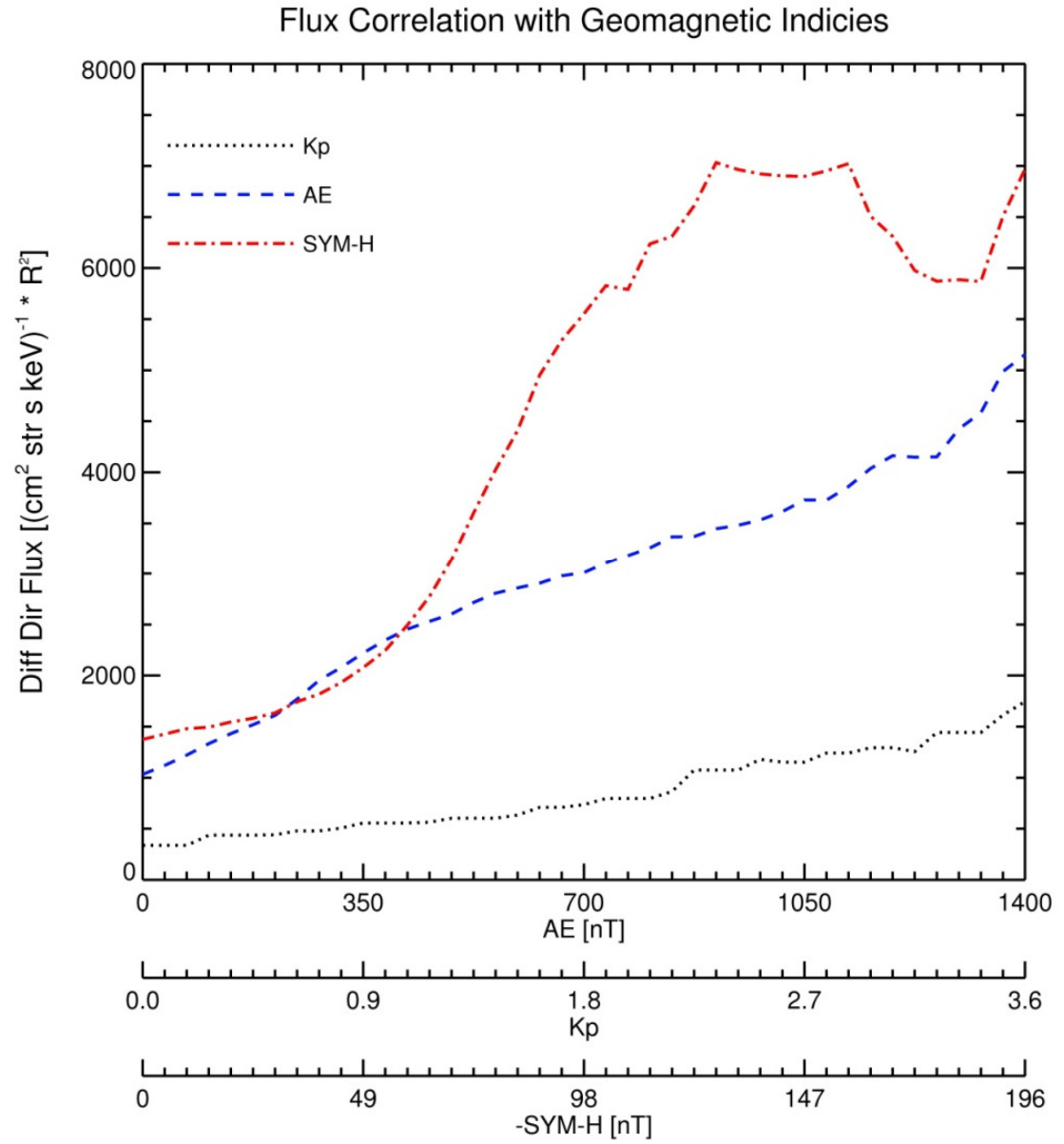
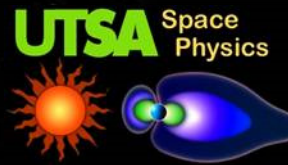
$IL_2 = 53.14^\circ$

% Diff: 13.7%



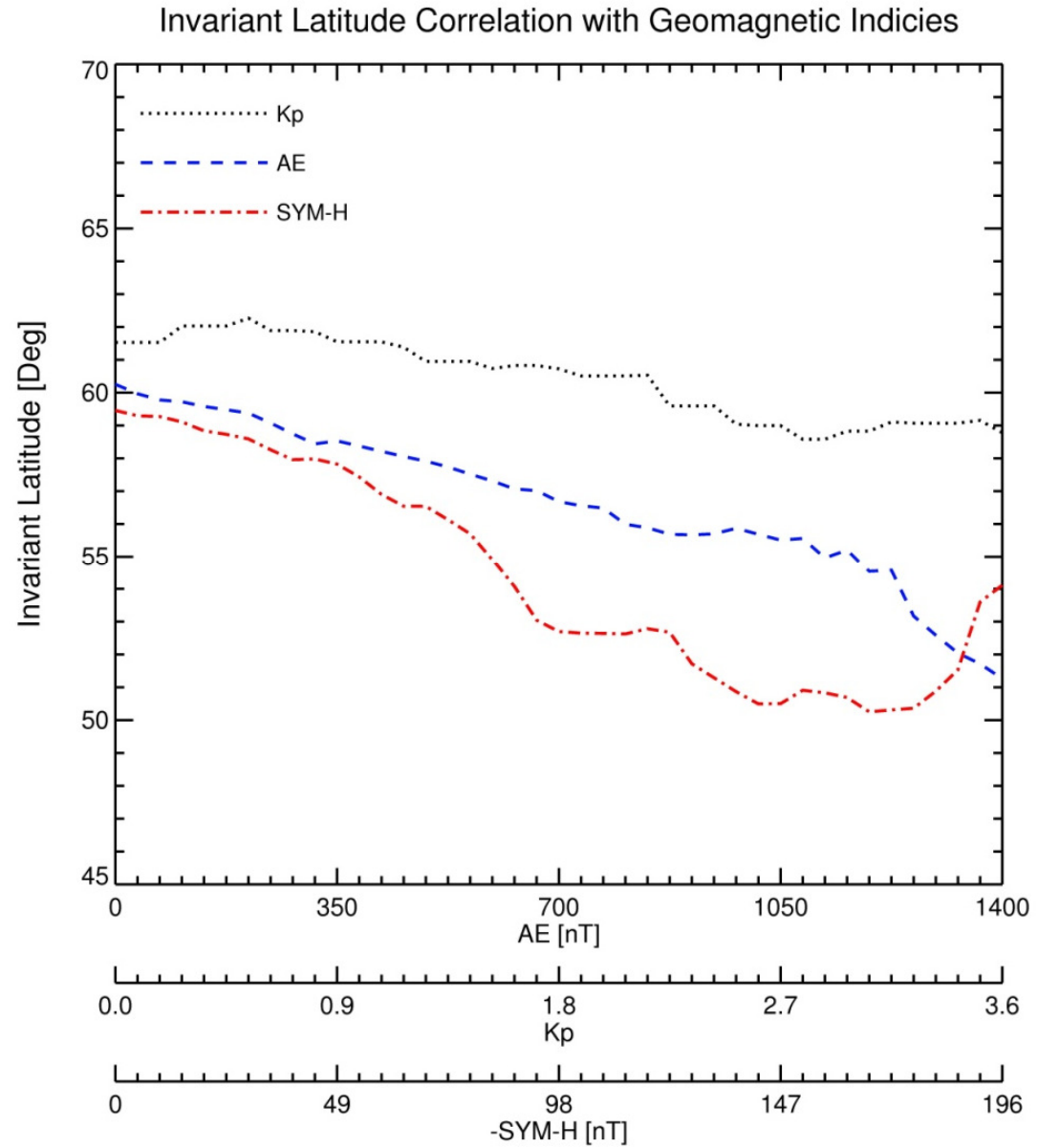
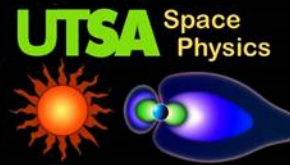


Flux Trendline



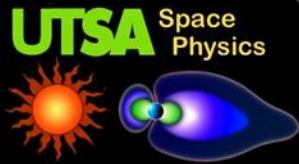


Invariant Latitude Trendline





Science Questions



- How is the ENA emission, from a point where ion energy is being precipitated, distributed in both ENA velocity space and configuration space?
- How is storm-time energy deposition from precipitating ions distributed in space (latitude, MLT) and how does that spatial dependence vary with geomagnetic storm phase?
- How much energy is deposited into the upper atmosphere by precipitating ring current particles during magnetic storms, as function of storm phase?